17 LIGHT-EMITTING DIODES

Roland H. Haitz, M. George Craford, and Robert H. Weissman
Hewlett-Packard Co.
San Jose, California

17.1 GLOSSARY

c	velocity of light
E_g	semiconductor energy bandgap
h	Planck' s constant
I_T	total LED current
J	LED current density
k	Boltzmann's constant
M	magnification
n_0	low index of refraction medium
n_1	high index of refraction medium
q	electron charge
T	temperature
V	applied voltage
η_i	internal quantum efficiency
θ_c	critical angle
λ	emission wavelength
τ	total minority carrier lifetime
τ_n	nonradiative minority carrier lifetime
τ_r	radiative minority carrier lifetime

17.2 INTRODUCTION

Over the past 25 years the light-emitting diode (LED) has grown from a laboratory curiosity to a broadly used light source for signaling applications. In 1992 LED production reached a level of approximately 25 billion chips, and $2.5 billion worth of LED-based components were shipped to original equipment manufacturers.

This chapter covers light-emitting diodes from the basic light-generation processes to descriptions of LED products. First, we will deal with light-generation mechanisms and light extraction. Four major types of device structures—from simple grown or diffused homojunctions to complex double heterojunction devices are discussed next, followed by a description of the commercially important semiconductors used for LEDs, from the pioneering GaAsP system to the AlGaInP system that is currently revolutionizing LED technology. Then processes used to fabricate LED chips are explained—the growth of GaAs and GaP substrates, the major techniques used for growing the epitixal material in which the light-generation processes occur, and the steps required to create LED chips up to the point of assembly. Next the important topics of quality and reliability—in particular, chip degradation and package-related failure mechanisms—will be addressed. Finally, LED-based products, such as indicator lamps, numeric and alphanumeric displays, optocouplers, fiber-optic transmitters, and sensors, are described.

This chapter covers the mainstream structures, materials, processes, and applications in use today. It does not cover certain advanced structures, such as quantum well or strained layer devices, a discussion of which can be found in Chap. 19, "Semiconductor Lasers." The reader is also referred to Chap. 19 for current information on edge-emitting LEDs, whose fabrication and use are similar to lasers.

For further information on the physics of light generation, the reader should consult Refs. 1 to 11. Semiconductor material systems for LEDs are discussed in Refs. 13 to 24. Crystal growth, epitaxial, and wafer fabrication processes are discussed in detail in Refs. 25 to 29.

17.3 LIGHT-GENERATION PROCESSES

When a *p-n* junction is biased in the forward direction, the resulting current flow across the boundary layer between the *p* and *n* regions has two components: holes are injected from the *p* region into the *n* region and electrons are injected from the *n* region into the *p* region. This so-called minority-carrier injection disturbs the carrier distribution from its equilibrium condition. The injected minority carriers recombine with majority carriers until thermal equilibrium is reestablished. As long as the current continues to flow, minority-carrier injection continues. On both sides of the junction, a new steady-state carrier distribution is established such that the recombination rate equals the injection rate.[1,2]

Minority-carrier recombination is not instantaneous. The injected minority carriers have to find proper conditions before the recombination process can take place. Both energy and momentum conservation have to be met. Energy conservation can be readily met since a photon can take up the energy of the electron-hole pair, but the photon doesn't contribute much to the conservation of momentum. Therefore, an electron can only combine with a hole of practically identical and opposite momentum. Such proper conditions are not readily met, resulting in a delay. In other words, the injected minority carrier has a finite lifetime τ_r before it combines radiatively through the emission of a photon.[2] This average time to recombine radiatively through the emission of light can be visualized as the average time it takes an injected minority carrier to find a majority carrier with the right momentum to allow radiative recombination without violating momentum conservation.

Unfortunately, radiative recombination is not the only recombination path. There are also crystalline defects, such as impurities, dislocations, surfaces, etc., that can trap the injected minority carriers. This type of recombination process may or may not generate light. Energy and momentum conservation are met through the successive emission of phonons. Again, the recombination process is not instantaneous because the minority carrier first has to diffuse to a recombination site. This nonradiative recombination process is characterized by a lifetime τ_n.[2]

Of primary interest in design of light-emitting diodes is the maximization of the radiative recombination relative to the nonradiative recombination. In other words, it is of interest to develop conditions where radiative recombination occurs fairly rapidly compared with nonradiative recombination. The effectiveness of the light-generation process is described by the fraction of the injected minority carriers that recombine radiatively compared to the total injection. The internal quantum efficiency η_i can be calculated from τ_r and τ. The combined recombination processes lead to a total minority-carrier lifetime τ given by Eq. (1):

$$\frac{1}{\tau}=\frac{1}{\tau_r}+\frac{1}{\tau_n} \tag{1}$$

η_i is simply computed from Eq. (1) as the fraction of carriers recombining radiatively:[2]

$$\eta_i=\frac{\tau_n}{\tau_r+\tau_n} \tag{2}$$

Of interest are two simple cases: in the case of excellent material quality (large τ_n) or efficient radiative recombination conditions (small τ_r), the internal quantum efficiency approaches 100 percent. For the opposite case ($\tau_n \ll \tau_r$), we find $\eta_i \approx \tau_n/\tau_r \ll 1$. As discussed under "Material Systems," there are several families of III–V compounds with internal quantum efficiencies approaching 100 percent. There are also other useful semiconductor materials with internal quantum efficiencies in the 1- to 10-percent range.

To find material systems for LEDs with a high quantum efficiency, one has to understand the band structure of semiconductors. The band structure describes the allowed distribution of energy and momentum states for electrons and holes (see Fig. 1 and Ref. 2). In practically all semiconductors the lower band, also known as the *valence band,* has a fairly simple structure, a

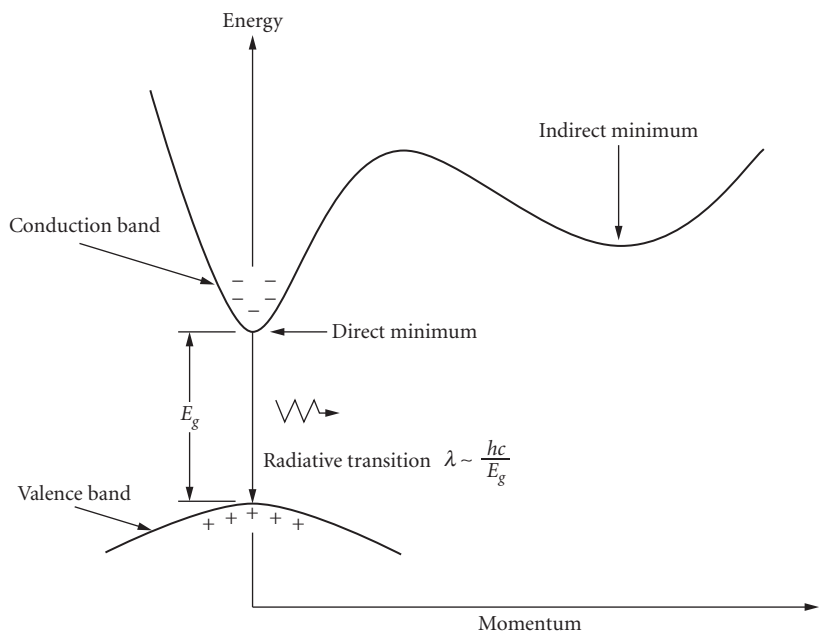

FIGURE 1 Energy band structure of a direct semiconductor showing radiative recombination of electrons in the conduction band with holes in the valence band.

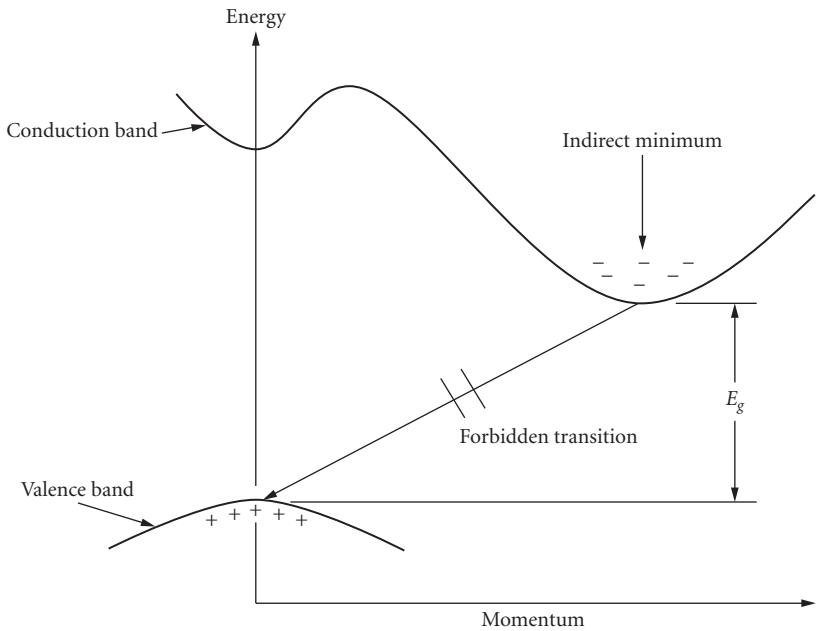

FIGURE 2 Energy band structure of an indirect semiconductor showing the conduction-band minima and valence-band maximum at different positions in momentum space. Radiative recombination of conduction-band electrons and valence-band holes is generally forbidden.

paraboloid around the $\langle 0, 0, 0 \rangle$ crystalline direction. Holes will take up a position near the apex of the paraboloid and have very small momentum. The upper band, also known as the *conduction band,* is different for various semiconductor materials. All semiconductors have multiple valleys in the conduction band. Of practical interest are the valleys with the lowest energy. Semiconductor materials are classified as either *direct* or *indirect.*[1–3] In a direct semiconductor, the lowest valley in the conduction band is directly above the apex of the valence-band paraboloid. In an indirect semiconductor, the lowest valleys are not at $\langle 0, 0, 0 \rangle$, but at different positions in momentum per energy space (see Fig. 2). Majority or minority carriers mostly occupy the lowest energy states, i.e., holes near the top of the valence band paraboloid and electrons near the bottom of the lowest conduction-band valley.

In the case of a direct semiconductor the electrons are positioned directly above the holes at the same momentum coordinates. It is relatively easy to match up electrons and holes with proper momentum-conserving conditions. Thus, the resulting radiative lifetime τ_r is short. On the other hand, electrons in an indirect valley will find it practically impossible to find momentum-matching holes and the resulting radiative lifetime will be long. Injected carriers in indirect material generally recombine nonradiatively through defects.

In a direct semiconductor, such as GaAs, the radiative lifetime τ_r is in the range of 1 to 100 ns, depending on doping, temperature, and other factors. It is relatively easy to grow crystals with sufficiently low defect density such that τ_n is in the same range as τ_r.

For indirect semiconductors, such as germanium or silicon, the radiative recombination process is extremely unlikely, and τ_r is in the range of seconds.[1] In this case, $\tau_r \gg \tau_n$, and practically all injected carriers recombine nonradiatively.

The wavelength of the photons emitted in a radiative recombination event is determined by the energy difference between the recombining electron-hole pair. Since carriers relax quickly to an energy level near the top of the valence band (holes), or the bottom of the conduction band

(electrons), we have the following approximation for the wavelength λ of the emitted photon (see Fig. 1):

$$\lambda \approx hc/E_g \tag{3}$$

where h = Planck' s constant, c = velocity of light, and E_g = bandgap energy.

This relation is only an approximation since holes and electrons are thermally distributed at levels slightly below the valence-band maximum and above the conduction-band minimum, resulting in a finite linewidth in the energy or wavelength of the emitted light. Another modification results from a recombination between a free electron and a hole trapped in a deep acceptor state. See Ref. 2 for a discussion of various recombination processes.

To change the wavelength or energy of the emitted light, one has to change the bandgap of the semiconductor material. For example, GaAs with a bandgap of 1.4 eV has an infrared emission wavelength of 900 nm. To achieve emission in the visible red region, the bandgap has to be raised to around 1.9 eV. This increase in E_g can be achieved by mixing GaAs with another material with a wider bandgap, for instance GaP with $E_g = 2.3$ eV. By adjusting the ratio of arsenic to phosphorous the bandgap of the resulting ternary compound, GaAsP, can be tailored to any value between 1.4 and 2.3 eV.[3]

The resulting band structure with varying As to P ratio is illustrated in Fig. 3. Note, the two conduction-band valleys do not move upward in energy space at the same rate. The direct valley moves up faster than the indirect valley with increasing phosphorous composition. At a composition of around 40 percent GaP and 60 percent GaAs, the direct and indirect valleys are about equal in energy. When the valleys are approximately equal in energy, electrons in the conduction band can scatter from the direct valley into the indirect valley. While the direct valley electrons still undergo rapid radiative recombination, the indirect valley electrons have a long radiative lifetime and either have to be scattered back to the direct valley or they will recombine nonradiatively. In other words, near this crossover

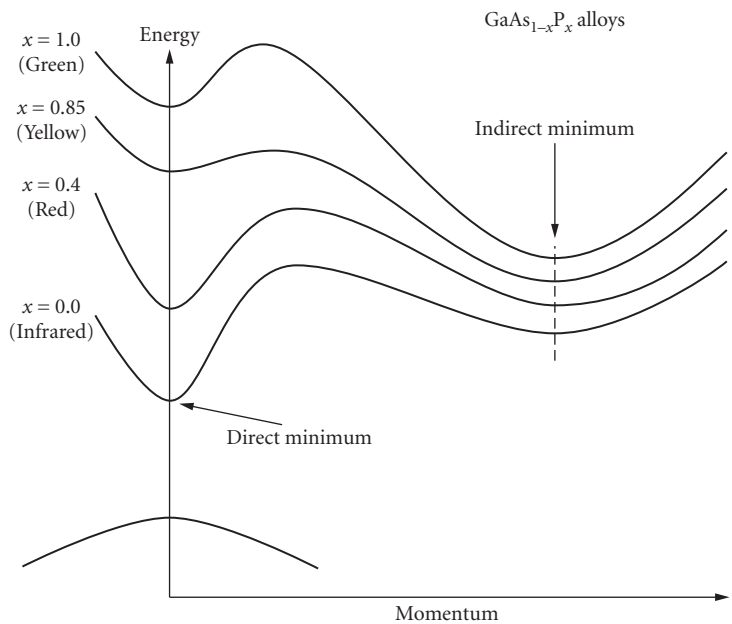

FIGURE 3 Energy band diagram for various alloys of the $GaAs_{1-x}P_x$ material system showing the direct and indirect conduction-band minima for various alloy compositions.

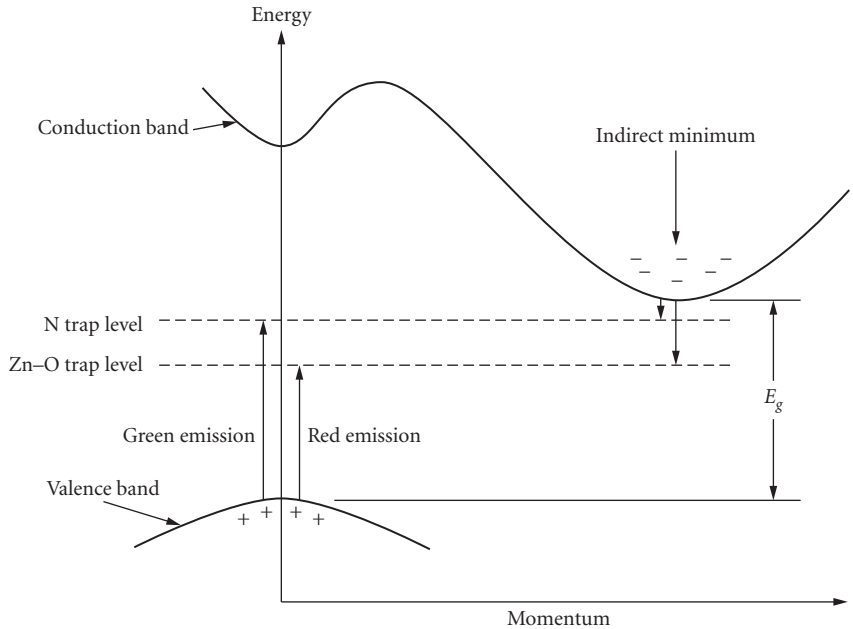

FIGURE 4 Formation of excitons (electron-hole pairs) by the addition of isoelectronic dopants N and ZnO to an indirect semiconductor. The excitons have a high probability to recombine radiatively.

between direct and indirect valleys, the radiative efficiency drops off dramatically, and for compositions with greater than 40 percent phosphorous the direct radiative recombination is practically nonexistent.[3,4]

The above discussion indicates that indirect semiconductors are not suitable for efficient generation of light through minority-carrier recombination. Fortunately, the introduction of so-called isoelectronic impurities can circumvent this limitation and introduces a new radiative recombination process.[5] A commonly used isoelectronic trap is generated by substituting a nitrogen atom for phosphorous in the GaAsP system[6–11] (see Fig. 4). Since N and P both have five electrons in their outer shell, the trap is electrically neutral. However, the stronger electronegativity of N relative to P can result in capture of an electron from the conduction band. Since the electron is very tightly bound to the impurity atom, its wave function in momentum space is spread out and has reasonable magnitude at $\langle k=0 \rangle$ in momentum space.[10] The negatively charged defect can attract a free hole to form a loosely bound electron-hole pair or "exciton." This electron-hole pair has a high probability to recombine radiatively. The energy of the emitted light is less than E_g. Another isoelectronic trap in GaP is formed by ZnO pairs (Zn on a Ga site and O on a P site) (see Fig. 4). The ZnO trap is deeper than the N trap, resulting in longer wavelength emission in the red region of the spectrum.[1]

The recombination process for exciton recombination is quite complex. For a detailed analysis, the reader is referred to Ref. 10. One result of this analysis is the recognition that the bound exciton has a relatively long lifetime in the range of 100 to 1000 ns. Light emission by exciton recombination is generally slower than emission due to direct band-to-band recombination.

17.4 LIGHT EXTRACTION

Generating light efficiently within a semiconductor material is only one part of the problem to build an efficient light source. The next challenge is the extraction of light from within the LED chip to the outside. The designer must consider total internal reflection.[1] According to Snell' s law, light can

escape from a medium of high index of refraction n_1 into a medium of low index refraction n_0 only if it intersects the surface between the two media at an angle from normal less than the critical angle θ_c with θ_c being defined by Eq. (4):

$$\theta_c = \text{arc sin}\, n_0/n_1 \tag{4}$$

Most semiconductor LEDs have an isotropic emission pattern as seen from within the light-generating material. Assuming a cubic shape for the LED chip, because of internal reflections, only a small fraction of the isotropically emitted light can escape any of the six surfaces. As a case in point, let us calculate the emission through the top surface. For typical light-emitting semiconductors, n_1 is in the range of 2.9 to 3.6. If $n_1 = 3.3$ and $n_0 = 1.0$ (air), we find $\theta_c = 17.6°$. The emission from an isotropic source into a cone with a half angle of θ_c is given by $(1 - \cos \theta_c)/2$. After correcting for Fresnel reflections, only 1.6 percent of the light generated escapes through the LED top surface into air. Depending on chip and *p-n* junction geometry, virtually all of the remaining light (98.4 percent) is reflected and absorbed within the LED chip.

The fraction of light coupled from chip to air is a function of the number of surfaces through which the chip can transmit light effectively. Most LED chips are called "absorbing substrate" (AS) chips. In such a chip, the starting substrate material (discussed later under "Substrate Technology") has a narrow bandgap and absorbs all the light with energy greater than the bandgap of the substrate. Consider the case of a GaAsP LED grown on a GaAs substrate. The emitted light (E_g>1.9eV) is absorbed by the GaAs substrate ($E_g = 1.4$ eV). Thus, a GaAsP-emitting layer on a GaAs substrate can transmit only through its top surface. Light transmitted toward the side surfaces or downward is absorbed.

To increase light extraction, the substrate or part of the epitaxial layers near the top of the chip has to be made of a material transparent to the emitted light. The "transparent substrate" (TS) chip is designed such that light transmitted toward the side surfaces within θ_c half-angle cones can escape. Assuming that there is negligible absorption between the point of light generation and the side walls, this increases the extraction efficiency by a factor of 5 (5 instead of 1 escape cones).

In a TS chip, additional light can be extracted if the side walls are nonplanar, i.e., if light from outside an escape cone can be scattered into an escape cone. This process increases the optical path within the chip and is very dependent on residual absorption. In a chip with low absorption and randomizing side surfaces, most of the light should escape. Unfortunately, in practical LED structures, there are several absorption mechanisms left such as front and back contacts, crystal defects, and absorption in areas where secondary radiative recombination is inefficient.

A common approach is to use a hybrid chip with properties between AS and TS chips. These chips utilize a thick, transparent window layer above the light-emitting layer. If this layer is sufficiently thick, then most of the light in the top half of the cones transmitted toward the side surfaces will reach the side of the chip before hitting the substrate. In this case of hybrid chips, the efficiency is between that of AS and TS chips as shown in Table 1.

Another important way to increase extraction efficiency is derived from a stepwise reduction in the index of refraction from chip to air. If the chip is first imbedded in a material with an intermediate index, i.e., plastic with $n_2 = 1.5$, then the critical angle θ_c between chip and plastic is increased to 27°. The extraction efficiency relative to air increases by the ratio of $(n_2/n_0)^2$ plus some additional correction for Fresnel-reflection losses. The gain from plastic encapsulation is usually around

TABLE 1 Extraction Efficiency into Air or Plastic for Three Types of Commonly Used LED Chips

		Typical extraction efficiency	
Chip Type	No. Cones	Air (%)	Plastic (%)
AS	1	1.5	4
Thick window	3	4.5	12
TS	5	7.5	20

2.7 times compared to air. Chips with multipath internal reflection will result in lower gains. It is important to note that this gain can be achieved only if the plastic/air interface can accommodate the increased angular distribution through proper lenslike surface shaping or efficient scattering optics. Table 1 illustrates the approximate extraction efficiencies achieved by the three dominant chip structures in air and in plastic. The numbers assume only first-pass extraction, limited absorption, and no multiple reflections within the chip.

17.5 DEVICE STRUCTURES

LED devices come in a broad range of structures. Each material system (see following section) requires a different optimization. The only common feature for all LED structures is the placement of the *p-n* junction where the light is generated. The *p-n* junction is practically never placed in the bulk-grown substrate material for the following reasons:

- The bulk-grown materials such as GaAs, GaP, and InP usually do not have the right energy gap for the desired wavelength of the emitted light.
- The light-generating region requires moderately low doping that is inconsistent with the need for a low series resistance.
- Bulk-grown material often has a relatively high defect density, making it difficult to achieve high efficiency.

Because of these reasons, practically all commercially important LED structures utilize a secondary growth step on top of a single-crystal bulk-grown substrate material. The secondary growth step consists of a single-crystal layer lattice matched to the substrate. This growth process is known as *epitaxial growth* and is described in a later section of this chapter.

The commonly used epitaxial structures can be classified into the following categories:

- Homojunctions
  - grown
  - diffused
- Heterojunctions
  - single confinement
  - double confinement

Grown Homojunctions

Figure 5 illustrates one of the simplest design approaches to an LED chip. An *n*-type GaAs layer with low to moderate doping density is grown on top of a highly doped *n*-type substrate by a vapor or liquid-phase epitaxial process (see "Epitaxial Technology"). After a growth of 5 to 10 μm, the doping is changed to *p* type for another 5 to 10 μm. A critical dimension is the thickness of the epitaxial *p* layer. The thickness should be larger than the diffusion length of electrons. In other words, the electrons should recombine radiatively in the epitaxially grown *p* layer before reaching the surface. The *p* layer should be of sufficiently high quality to meet the condition for efficient recombination, i.e., $\tau_n \gg \tau_r$. In addition, the side surfaces may have to be etched to remove damage. Damage and other defects where the *p-n* junction intercepts the chip surface can lead to a substantial leakage current that reduces efficiency, especially at low drive levels.

The structure of Fig. 5 was used in some of the earliest infrared emitters (wavelength 900 nm). Efficiency was low, typically 1 percent. Modern infrared emitters use Si-doped GaAs (see Fig. 6). The detailed recombination mechanism in GaAs:Si even today is quite controversial and goes beyond the scope of this publication. The recombination process has two important characteristics: (1) the radiative lifetime τ_r is relatively slow, i.e., in the range of 1 μs and (2) the wavelength is shifted to 940 nm.

LIGHT-EMITTING DIODES

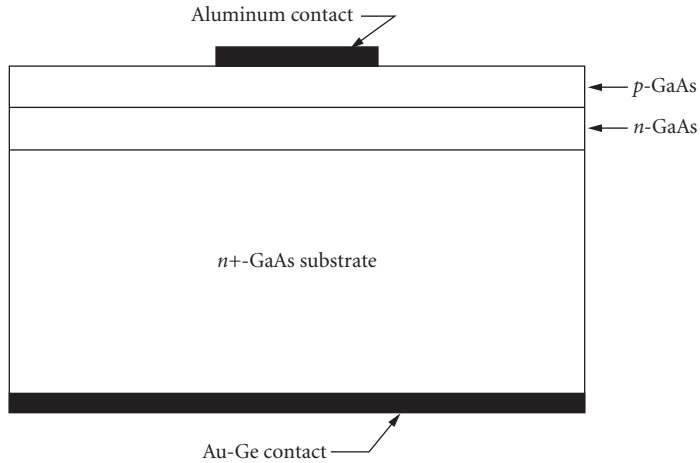

FIGURE 5 Cross section of an infrared LED chip. A *p-n* junction is formed by epitaxially growing *n*- and *p*-doped GaAs onto an n+-doped GaAs substrate.

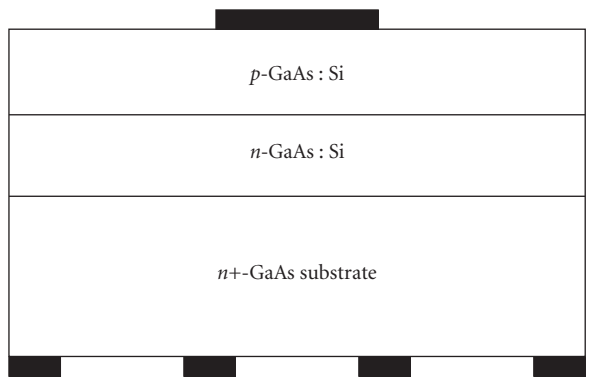

FIGURE 6 A high-efficiency IR LED made by LPE growth of GaAs that is doped with silicon on both the *p* and *n* sides of the junction. To increase external quantum efficiency, a partly reflective back contact is employed.

At this wavelength the GaAs substrate is partly transparent, making this device a quasi-TS structure with efficiencies into plastic of 5 to 10 percent.

Diffused Homojunction

The chip structure of Fig. 5 can also be produced by a zinc (Zn) diffusion into a thick *n* layer. The commercially most significant structure of this type is shown in Fig. 7. By replacing 40 percent of the As atoms with P atoms, the bandgap is increased to 1.92 eV to make a GaAsP LED that emits visible red light. In this case, the *p-n* junction is diffused selectively by using a deposited layer of silicon-nitride as a diffusion mask. This structure of Fig. 7 has several advantages over the structure of Fig. 5. Lateral diffusion of Zn moves the intersection of the junction with the chip surface

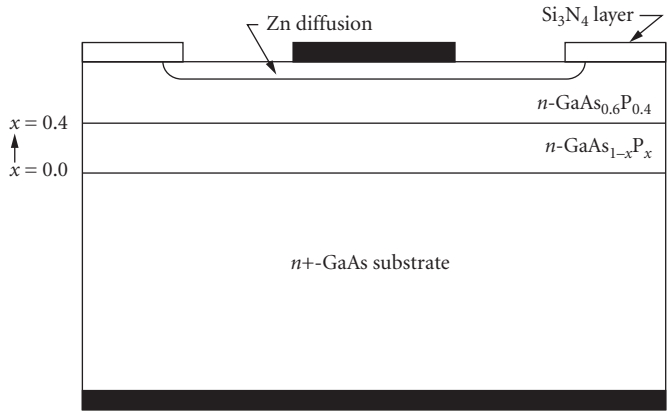

FIGURE 7 GaAsP LED which emits at 650 nm. On a GaAs substrate, a layer is grown whose composition varies linearly from GaAs to $GaAs_{0.6}P_{0.4}$, followed by a layer of constant composition. Zinc is selectively diffused using an Si_3N_4 mask to form the light-emitting junction.

underneath the protecting Si_3N_4 layer. This layer protects the junction from contamination and adds to the long-term stability of the device. In addition, it is important for applications requiring more than one clearly separated light-emitting area. For instance, seven-segment displays, such as those used in the early handheld calculators, are made by diffusing seven long and narrow stripes into a single chip of GaAsP material. (See Fig. 8.) This chip consists of eight (seven segments plus decimal point) individually addressable *p*-regions (anodes) with a common *n*-type cathode. Such a chip is feasible only in an AS-type structure because the individual segments have to be optically isolated from each other. A TS-type structure results in unacceptable levels of crosstalk.

Figure 7 shows another feature of practical LED devices. The composition with 40 percent P and 60 percent As has a lattice constant (atomic spacing) that is different from the GaAs substrate. Such a lattice mismatch between adjacent layers would result in a very high density of dislocations. To reduce this problem to an acceptable level, one has to slowly increase the phosphorous composition from 0 percent at the GaAs interface to 40 percent over a 10- to 20-μm-thick buffer layer. Typically, the buffer layer is graded linearly. The phosphorous composition is increased linearly from bottom to top. The thicker the buffer layer, the lower is the resulting dislocation density. Cost constraints keep the layer in the 10- to 15-μm range. The layer of constant composition (40 percent P) has to be thick enough to accommodate the Zn diffusion plus the diffusion length of minority carriers. A thickness range of 5 to 10 μm is typical.

Another variation of a homojunction is shown in the TS-chip structure of Fig. 9. Instead of an absorbing GaAs substrate, one starts with a transparent GaP substrate. The graded layer has an inverse gradient relative to the chip shown in Fig. 7. The initial growth is 100 percent GaP phasing in As linearly over 10 to 15 μm. At 15 percent As, the emission is in the yellow range (585 nm), at 25 percent in the orange range (605 nm), and at 35 percent in the red range (635 nm). Figure 3 shows the approximate band structure of this material system. The composition range mentioned above has an indirect band structure. To obtain efficient light emission, the region of minority-carrier injection is doped with nitrogen forming an isoelectronic recombination center (see exciton recombination in the first section).

Figure 9 shows an important technique to increase extraction efficiency. In a TS-chip, the major light loss is due to free carrier absorption at the alloyed contacts. Rather than covering the entire bottom surface of the chip with contact metal, one can reduce the contact area either by depositing small contact islands (see Fig. 6) or by placing a dielectric mirror (deposited SiO_2) between the substrate and the unused areas of the back contact (Fig. 9). This dielectric mirror increases the efficiency by 20 to 50 percent at the expense of higher manufacturing cost.

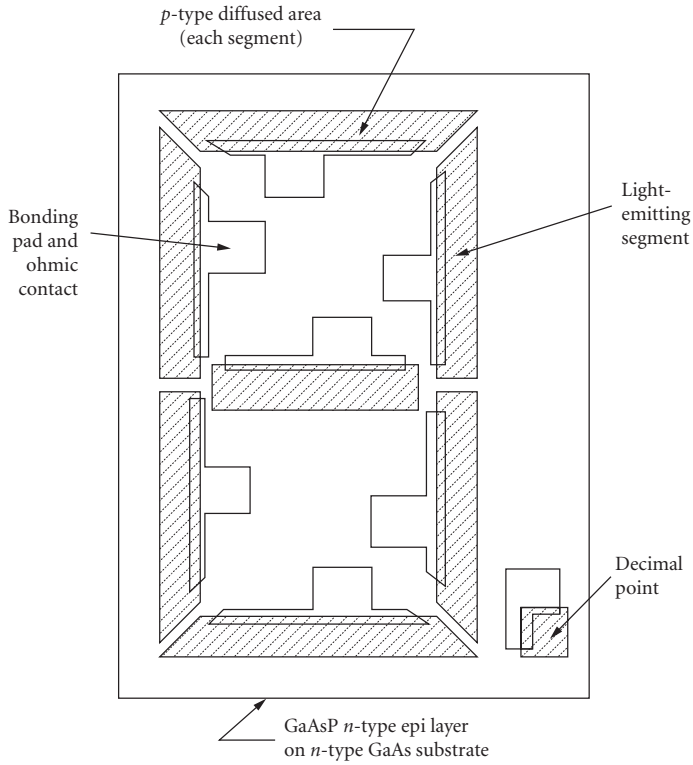

FIGURE 8 Monolithic seven-segment display chip with eight separate diffused regions (anodes) and a common cathode (the GaAs substrate).

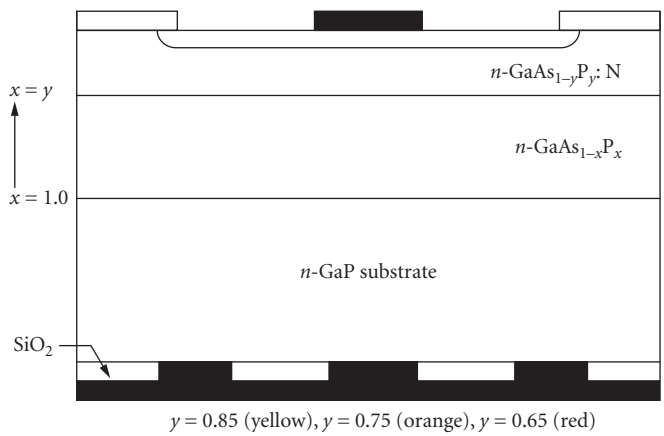

FIGURE 9 Cross section of a $GaAs_{1-x}P_x$ LED which, by changing the composition "x," produces red, orange, or yellow light. The top layer is doped with nitrogen to increase the quantum efficiency. The GaP substrate is transparent to the emitted light. Also shown is a reflective back contact made by depositing the contact metallization on top of SiO_2.

Single Heterojunctions

Heterojunctions introduce a new variable: local variation of the energy bandgap resulting in carrier confinement. Figure 10 shows a popular structure for a red LED emitter chip. A *p*-type layer of GaAlAs with 38 percent Al is grown on a GaAs substrate. The GaAlAs alloy system can be lattice-matched to GaAs; therefore, no graded layer is required as in the GaAsP system of Fig. 7. Next, an *n*-type layer is grown with 75 percent Al. The variation of E_g from substrate to top is illustrated in Fig. 11. Holes accumulate in the GaAlAs *p* layer with the narrower bandgap. Electrons are injected from the *n* layer into this *p* layer. The holes have insufficient energy to climb the potential barrier into the wide-bandgap material. Holes are confined to the *p* layer. In the *p* layer, the radiative recombination time is very short because of the high concentration of holes. As a result, the internal quantum efficiency is quite high. A variation of this structure is a widely used infrared emitter that emits at 880 nm.

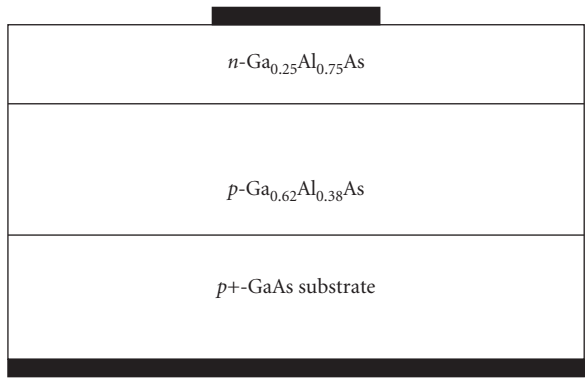

FIGURE 10 Cross section of a single heterostructure LED.

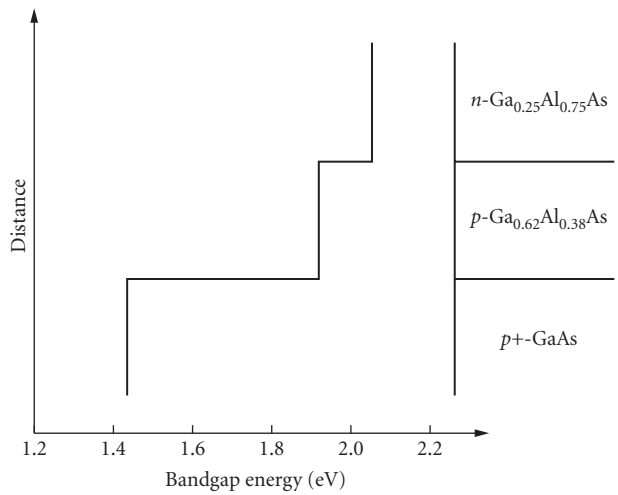

FIGURE 11 Variation in energy bandgap for the various layers in the GaAlAs LED shown in Fig. 10.

Double Heterostructures

The double heterostructure shown in Fig. 12 repeats the *p*-side confinement of Fig. 10 on the *n* side. An *n*-type buffer layer is grown on the GaAs substrate to create a high-quality surface onto which the first *n*-type GaAlAs confinement layer with 75 percent Al is grown. The active or light-generation layer is a 3-μm-thick *p*-type layer with 38 percent Al. The top *p*-type confinement layer again uses 75 percent Al. This structure with the energy-band diagram of Fig. 13 has two advantages: (1) There is no hole injection into the *n*-type layer with reduced efficiency and a slow hole recombination in the lowly doped *n* layer. (2) The high electron and hole density in the active layer reduces τ_r, thus increasing device speed and efficiency. The increased speed is quite important for LED sources in fiber-optic communication applications. (See "Fiber Optics" subsection later in this chapter.)

The double heterostructure of Fig. 12 represents a one-dimensional containment of injected carriers. Injection and light emission occurs across the entire lateral dimension of the chip. For fiber-optic applications, the light generated over such a large area cannot be effectively coupled into small-diameter fiber. A rule of thumb for fiber coupling requires that the light-emitting area be equal to or, preferably, smaller than the fiber core diameter. This rule requires lateral constraint of carrier injection. The localized diffusion of Fig. 7 is not applicable to grown structures such as those in Fig. 12. The preferred solution inserts an *n* layer between buffer and lower confinement layer (see Fig. 14). A hole etched into the *n* layer allows current flow. Outside of this hole, the *p*-*n* junction between *n* layer and lower confinement layer is reverse-biased, thus blocking any current flow. The disadvantage of this approach is a complication of the growth process. In a first growth process, the *n* layer is grown. Then a hole is etched into the *n* layer using standard photolithographic etching techniques. Finally, a second epitaxial growth is used for the remaining layers.

Another technique to constrain current injection utilizes a small ohmic contact.[12] It is used frequently in conjunction with InP-based fiber-optic emitters (see Fig. 15). An SiO_2 layer limits contact to a small-diameter (typically 25 μm) hole that results in a relatively small light-emitting area. The etched lens shown for this structure helps to collimate the light for more efficient coupling onto the fiber.[12]

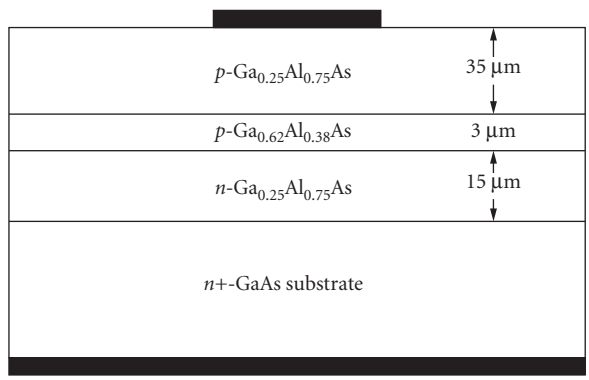

FIGURE 12 Structure of a double heterostructure (DH) GaAlAs LED. The DH is composed of a $Ga_{0.62}Al_{0.38}As$ layer surrounded on either side by a $Ga_{0.25}Al_{0.75}As$ layer. The thick top layer acts as window to increase light extraction through the side walls of the chip.

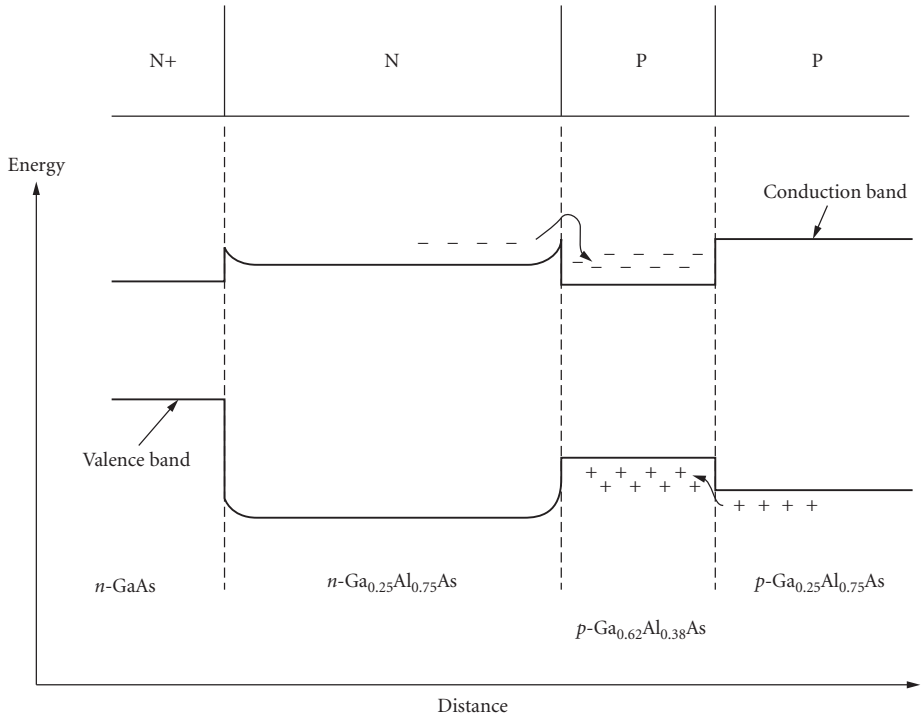

FIGURE 13 Energy band diagram of the GaAlAs LED shown in Fig. 12. The LED is forward biased. Electrons and holes are confined in the *p*-doped $Ga_{0.62}Al_{0.38}As$ layer, which increases the radiative recombination efficiency.

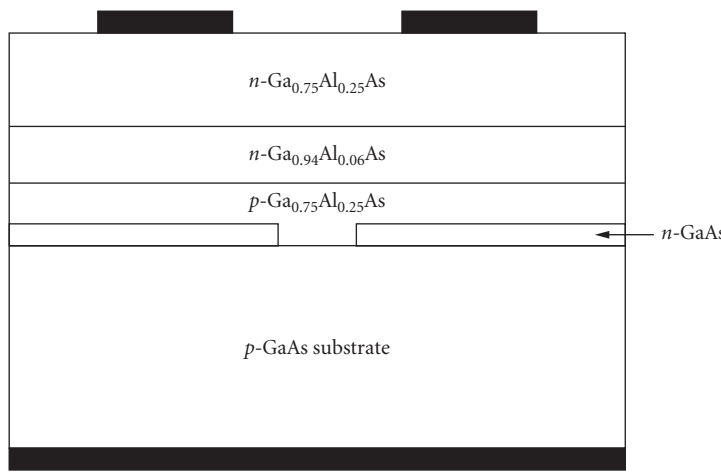

FIGURE 14 Cross section of an LED with three-dimensional carrier confinement. A DH structure is used to confine injected carriers in the $Ga_{0.94}Al_{0.06}As$ layer (direction perpendicular to the junction). The patterned, *n*-type GaAs layer is used to limit current flow in the lateral direction. The small emitting area and the 820-nm emission of this LED makes it ideal for fiber-optic applications.

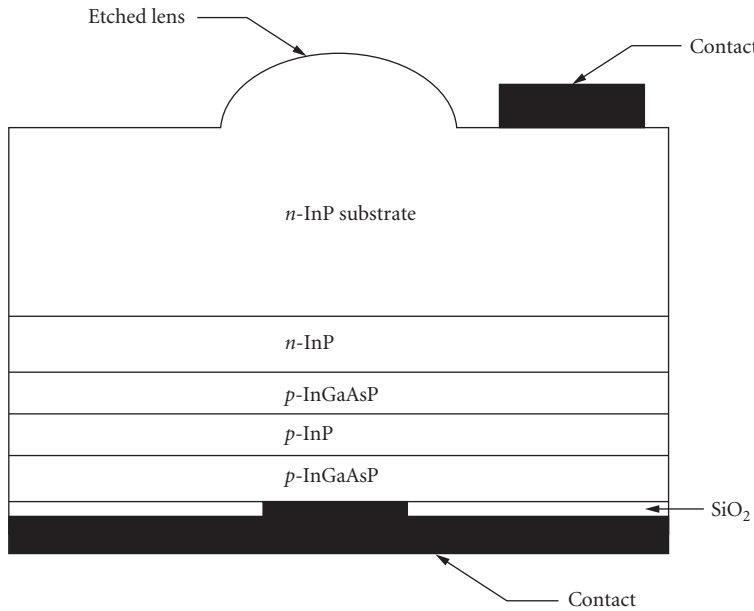

FIGURE 15 Structure of a 1300-nm LED used for optical fiber communications. The cross section shows the DH-layer configuration, limited area back contact for emission-size control, and an etched lens at the top of the chip which, magnifies ($M = 2$) the source area and collimates the light for effective coupling into a fiber.

17.6 MATERIAL SYSTEMS

The $GaAs_{1-x}P_x$ System

The most widely used alloy for LEDs is the ternary $GaAs_{1-x}P_x$ system, including its two binary components GaAs and GaP. This system is best described by the composition parameter x with $0 \le x \le 1$. For $x = 0$, we have GaAs and for $x = 1$ the composition is GaP. For $x \le 0.4$, the alloy has a direct bandgap. GaAs was developed in the early 1960s as an infrared emitter with a wavelength of 910 nm and an efficiency in the range of 1 percent. This emitter was soon followed by a Si-doped variety. As discussed earlier, this leads to an emission wavelength of 940 nm, a wavelength at which the GaAs substrate is partly transparent. The resulting efficiency is increased substantially and, depending on configuration, is in the 5- to 10-percent range. However, the recombination process is quite slow, resulting in rise and fall times in the 50-ns to 1.0-μs range (see Table 2). One other drawback is caused by the low absorption coefficient of Si detectors at 940 nm. To absorb 90 percent of the light requires a detector thickness of 60 to 70 μm. Conventional photo transistors are quite suitable as detectors. Integrated photo ICs with their 5- to 7-μm-thick epitaxial layers are very inefficient as detectors at 940 nm.

To shift the wavelength toward the near-infrared or into the visible spectrum, one has to grow a ternary alloy, a mixture between GaAs and GaP. Of commercial interest are two alloys with $x = 0.3$ and $x = 0.4$ grown on a GaAs substrate (see Table 2). The $x = 0.4$ alloy was the first commercially produced material with a wavelength in the visible range of the spectrum. Grown on an absorbing substrate, it has a modest luminous efficacy of around 0.2 lm/A. [Luminous efficacy is the luminous (visible) flux output measured in lumens divided by the electrical current input.] The absorbing substrate allows the integration of multiple light sources into a single chip without crosstalk. Such

TABLE 2 Performance Summary of LED Chips in the $GaAs_{1-x}P_x$ System

x	Growth Process*	Isoel. Dopant	Substrate†	Dominant Wavelength (nm)	Colon‡	Luminous Efficacy§ (lm/A)	Quantum Efficiency§ (%)	Speed (ns)
0	LPE	—	AS	910	IR		1	50
0	LPE	—	TS	940	IR		10	1000
0.3	VPE	—	AS	700	IR		0.5	50
0.4	VPE	—	AS	650	Red	0.2		50
0.65	VPE	N	TS	635	Red	2.5		300
0.75	VPE	N	TS	605	Orange	2.5		300
0.85	VPE	N	TS	585	Yellow	2.5		300
1.0	LPE	N	TS	572	Y/green	6		300
1.0	LPE	—	TS	565	Green	1		
1.0	LPE	ZnO	TS	640	Red	1		

*LPE = liquid phase epitaxy; VPE = vapor phase epitaxy.
†AS = absorbing substrate; TS = transparent substrate.
‡IR = infrared.
§Into plastic (index = 1.5).

monolithic seven-segment displays became the workhorse display technology for handheld calculators from 1972 to 1976.[9,13] Today this alloy is used in LED arrays for printers.[14]

The $x = 0.3$ alloy with a wavelength of 700 nm became important in the mid 1970s as a light source in applications using integrated photodetectors. It has 3 to 5 times the quantum efficiency of the $x = 0.4$ alloy (see Table 2), but has a lower luminous efficacy because of the much-reduced eye sensitivity at 700 nm.

For $x > 0.4$, the GaAsP material system becomes indirect (see earlier under "Light-Generation Processes" and Fig. 3). The quantum efficiency decreases faster than the increase in eye sensitivity.[4] The only way to achieve a meaningful efficiency is through the use of isoelectronic dopants as described earlier. The choices for isoelectronic dopants that have been successful are N for GaAsP[11] and N or ZnO for GaP. Nitrogen doping is used widely for alloys with $x = 0.65$ to $x = 1.0$.[6–10] The resulting light sources cover the wavelength range from 635 nm to approximately 565 nm (see Table 2). Since these alloys are either GaP or very close in composition to GaP, they are all grown on GaP substrates. The resulting transparent-substrate chip structure increases the luminous efficacy.

In the case of the binary GaP compound, the dominant wavelength depends on N concentration. With low concentrations, practically all N atoms are isolated in single sites. With increasing concentration, N atoms can arrange themselves as pairs or triplets. The resulting electron traps have lower energy states, which shift the emitted light toward longer wavelength. Phonon coupling can also reduce the emission energy. Commercially significant are two compositions: (1) undoped GaP which emits at 565 nm (dominant wavelength) with a reasonably green appearance and a low efficiency of around 1 lm/A, and (2) GaP with a nitrogen concentration in the range of 10^{19} cm^{-3} with a substantially higher luminous efficiency of around 6 lm/A at 572 nm. At this wavelength, the color appearance is yellow-green, often described as chartreuse.

Three nitrogen-doped ternary alloys of GaAsP are commercially important for red, orange, and yellow. The red source with $x = 0.65$ has an efficiency in the range of 2 to 3 lm/A. With increasing bandgap or decreasing wavelength, the drop in quantum efficiency is compensated by an increase in eye sensitivity, resulting in a practically wavelength-independent luminous efficiency for the range of 635 to 585 nm.[8,15]

ZnO-doped GaP is an interesting material. The quantum efficiency of such chips is relatively high, around 3 percent. However, the linewidth is quite broad. The quantum efficiency peaks at 700 nm, but the luminous efficiency peaks at 640 nm (dominant wavelength). In other words, most of the photons are emitted at wavelengths with low eye sensitivity. Another problem of GaP:ZnO is saturation. The deep ZnO electron trap causes very slow exciton recombination. At high injection currents, all traps are saturated and most of the injected carriers recombine

nonradiatively. At low injection levels (≤1 A/cm^2), the efficacy is relatively high, 3 to 5 lm/A. At a more useful density of 10 to 30 A/cm^2, the emission saturates, resulting in an efficacy of around 1 lm/A.

The $Al_xGa_{1-x}As$ System

The $Al_xGa_{1-x}As$ material system has a direct bandgap for $0 \le x \le 0.38$. This system has one very significant advantage over the GaAsP system described earlier, the entire alloy range from $x = 0$ to $x = 1$ can be lattice-matched to GaAs. In other words, every alloy composition can be directly grown on any other alloy composition without the need for transition layers. This feature allows the growth of very abrupt heterojunctions, i.e., abrupt transition in composition and bandgap. These heterojunctions add one important property not available in the GaAsP system: carrier containment (see earlier under "Device Structures"). Carrier containment reduces the movement of injected carriers in a direction perpendicular to the junction. Thus, carrier density can be increased beyond the diffusion-limited levels. This results in increased internal quantum efficiency and higher speed. Another benefit is reduced absorption and improved extraction efficiency (under "Light Extraction").

Of practical significance are two compositions: $x = 0.06$ and $x = 0.38$ (see Table 3). Both compositions exist in single and double heterojunction variations (see under "Device Structures"). The double heterojunctions usually have a 1.5 to 2.0 times advantage in efficiency and speed. In all cases, the efficiency strongly depends on the thickness of the window layer and, to a lesser degree, on the thickness of the transparent layer between active layer and absorbing substrate (see Fig. 12). Chips with a transparent substrate have an additional efficiency improvement of 1.5 to 3.0 times again, depending on layer thickness and contact area. The efficiency variation is best understood by counting exit cones as described in the text in conjunction with Table 1. For $x = 0.06$, the internal quantum efficiency of a double heterojunction approaches 100 percent. For $x = 0.38$, the direct and indirect valleys are practically at the same level and the internal quantum efficiency is reduced to the range of 50 percent, again dependent upon the quality of the manufacturing process.

The best compromise for efficiency and speed is the $x = 0.06$ alloy as a double heterostructure. Depending on layer thickness, substrate, and contact area, these devices have efficiencies of 5 to 20 percent and rise/fall times of 20 to 50 ns. This alloy is becoming the workhorse for all infrared applications demanding power and speed. A structural variation as shown in Fig. 14 is an important light source for fiber-optic communication.

The $x = 0.38$ alloy is optimized for applications in the visible spectrum. The highest product of quantum efficiency and eye response is achieved at $x = 0.38$ and $\lambda = 650$ nm. The single heterostructure on an absorbing substrate has an efficacy of around 4 lm/A. The equivalent double heterostructure is in the 6- to 8-lm/A range. On a transparent GaAlAs substrate, the efficacy is typically in the 15- to 20-lm/A range and results of as high as 30 lm/A have been reported in the literature.[16] The major application for these red LEDs is in light-flux-intensive applications, such as message panels and automotive stoplights. A variation optimized for speed is widely used for optical communication using plastic fiber.

TABLE 3 Performance Summary of LED Chips in the $Al_xGa_{1-x}As$ System

x	λ (nm)	Substrate*	Structure†	Efficiency or Efficacy	Speed (ns)
0.06	820	AS, TW	DH	8%	30
0.06	820	TS	DH	15%	30
0.38	650	AS, TW	SH	4 lm/A	
0.38	650	AS, TW	DH	8 lm/A	
0.38	650	TS	DH	16 lm/A	

*AS = absorbing substrate; TW = thick window layer; TS = transport substrate.
†DH = double heterostructure; SH = single heterostructure.

The AlInGaP System

The AlInGaP system has most of the advantages of the AlGaAs system with the additional advantage that it has a higher-energy direct energy gap of 2.3 eV that corresponds to green emission at 540 nm. AlInGaP can be lattice-matched to GaAs substrates. Indium occupies about half of the Group III atomic sites. The ratio of aluminum to gallium can be changed without affecting the lattice match, just as it can in the AlGaAs material system, since A1P and GaP have nearly the same lattice spacing. This enables the growth of heterostructures that have the efficiency advantages described in the previous section.

Various AlInGaP device structures have been grown. A simple DH structure with an AlInGaP active layer surrounded by higher bandgap AlInGaP confining layers has been effective for injection lasers, but has not produced efficient surface-emitting LEDs.[17] The main problem has been that AlInGaP is relatively resistive and the top AlInGaP layer is not effective in distributing the current uniformly over the chip. This is not a problem with lasers since the top surface is covered with metal and the light is emitted from the edge of the chip.

The top layer must also be transparent to the light that is generated. Two window layers used are AlGaAs or GaP on top of the AlInGaP heterostructure.[18,19] AlGaAs has the advantage that it is lattice-matched and introduces a minimum number of defects at the interface, but it has the disadvantage that it is somewhat absorptive to the yellow and green light which is generated for high-aluminum compositions. The highest AlInGaP device efficiencies have been achieved using GaP window layers.[18,20] GaP has the advantage that it is transparent to shorter wavelengths than AlGaAs and that it is easy to grow thick GaP layers, using either VPE or LPE, on top of the AlInGaP DH that was grown by MOVPE. Both VPE and LPE have substantially higher growth rates than MOCVD. The various growth techniques are discussed later under "Epitaxial Technology."

AlInGaP devices with 45-μm-thick GaP window layers have achieved external quantum efficiencies exceeding 5 percent in the red and yellow regions of the emission spectrum.[21] This is more than twice as bright as devices that have thinner AlGaAs window layers.

Green-emitting AlInGaP devices have also been grown which are brighter than the conventional GaP and GaP:N green emitters.[18,20,21] Substantial further improvement in green is expected since the quantum efficiency is not as high as would be expected based on the energy position of the transition from a direct to an indirect semiconductor.

The performance of AlInGaP LEDs compared to the most important other types of visible emitters is shown in Figs. 16 and 17. GaAsP on a GaAs substrate and GaP: ZnO are not shown since their luminous efficacy are off the chart at the bottom and the lower-right-hand corner, respectively. It is clear from Fig. 17 that the luminous efficacy of AlInGaP is substantially higher than the other technologies in all color regions except for red beyond 640 nm. Since forward voltage is typically about 2 V, the lumen per watt value for a given device is about one-half the lumen per ampere value that is given in Tables 2 and 3. The quantum efficiency of AlInGaP is also better than all of the other technologies except for the highest-performance AlGaAs devices operating at about 650 nm. Because of the eye sensitivity variations (see C.I.E. curve in Fig. 16), the 620 nm (red/orange) AlInGaP devices have a higher luminous efficiacy than 650 nm AlGaAs LEDs (see Fig. 17).

Blue LED Technology

Blue emitters have been commercially available for more than a decade, but have only begun to have a significant impact on the market in the last few years. SiC is the leading technology for blue emitters with a quantum efficiency of about 0.02 percent and 0.04 lm/A luminous performance. SiC devices are not much used due to their high price and relatively low performance efficiency.

Other approaches for making blue LEDs are the use of II–VI compounds such as ZnSe or the nitride system GaN, AlGaN, or AlGaInN. It has been difficult to make good *p-n* junctions in these materials. Recently improved *p-n* junctions have been demonstrated in both ZnSe[22,23] and GaN.[24]

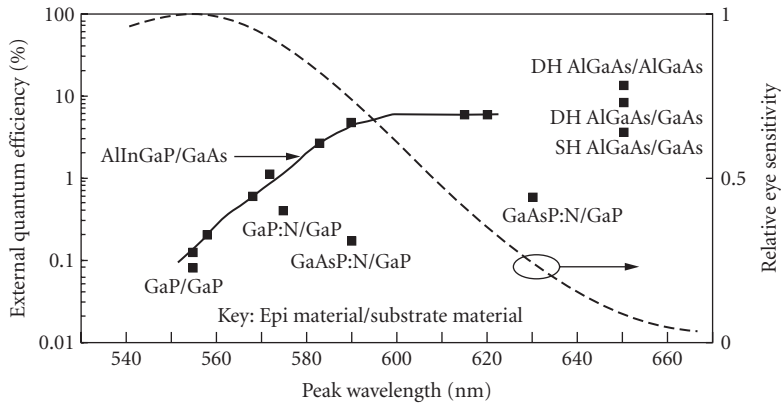

FIGURE 16 External quantum efficiency as a function of peak wavelength for various types of visible LEDs. Below 590 nm the efficiency of AlInGaP LEDs decreases due to the approaching transition from direct to indirect semiconductor. The human eye sensitivity curve is also shown. Since the eye response increases sharply from 660 to 540 nm, it partially makes up for the drop in AlInGaP LED efficiency. The resulting luminous performance is shown in Fig. 17.

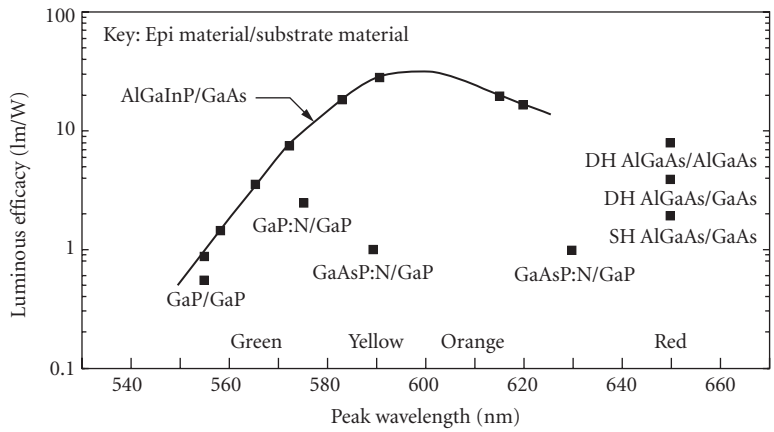

FIGURE 17 Luminous efficacy for AlInGaP LEDs versus wavelength compared to other LED technologies. AlInGaP LEDs are more than an order of magnitude brighter in the orange and yellow regions than other LEDs. AlInGaP LEDs compare favorably to the best AlGaAs red LEDs.

Device performance is still in the 0.1-lm/A range and reliability is unproven. However, this recent progress is very encouraging for blue-emission technology and could lead to a high-performance device in the next few years. Both ZnSe and the nitride system have a major advantage over SiC because they are direct bandgap semiconductors, so a much higher internal quantum efficiency is possible. However, it is difficult to find suitable lattice-matched substrates for these materials.

17.7 SUBSTRATE TECHNOLOGY

Substrate Criteria

There are several requirements for substrates for LEDs. The substrate must be as conductive as possible both thermally and electrically to minimize power loss. In order to minimize defects it should match the epitaxial layers as closely as possible in atomic lattice spacing, and in the coefficient of thermal expansion. The substrate should also have a low defect density itself. Finally, the substrate should, if possible, be transparent to the light generated by the LED structure since this will enhance the external quantum efficiency.

Substrate Choices

The substrates used for nearly all visible LEDs are GaAs and GaP. GaAs or InP is used for infrared devices, depending upon the device structure required. Substrate parameters are summarized in Table 4, along with Si and Ge for comparison. GaAs is used for the AlGaAs and AlInGaP material systems since they can be lattice-matched to it. GaAs is also used for the $GaAs_{1-x}P_x$, system for $x \leq 0.4$ because it is more nearly latticed-matched and, since it is absorbing, it is useful in multiple-junction devices where optical crosstalk must be minimized (see under "Diffused Homojunction" and Fig. 8). GaP is used for compositions of $x > 0.6$ due to its transparency and closer lattice match. However, neither GaP nor GaAs are well matched to GaAsP, and grading layers are required to grow epitaxial layers with decent quality. InP is the choice for long wavelength emitters made using the InGaAs or InGaAsP materials systems, due to the better lattice match.

Substrate Doping

Generally, substrates are *n* type and are doped with Te, S, or Si, although sometimes Se and Sn are also used. In some cases, particularly for some AlGaAs LEDs and laser structures, *p*-type substrates are required and Zn is nearly always the dopant. The doping levels are typically in the 10^{18}-cm^{-3} range. Basically, the substrates are doped as heavily as possible to maximize conductivity. However, the doping must be below the solubility limit to eliminate precipitates and other defects. In the case of substrates that are transparent to the light which is generated, such as GaP, with a $GaAs_{1-x}P_x$ epitaxial layer, the doping should also remain below the level at which substantial free carrier absorption occurs.

Growth Techniques

Substrates can be grown by either the Bridgeman or Liquid Encapsulated Czochralski (LEC) technique. The LEC technique is the most widely used. Both techniques are described in detail elsewhere and will be only briefly summarized here.[25]

TABLE 4 Properties of Common Semiconductor Substrates

Substrate	Lattice Parameter	Energy Gap @ 300 K (eV)		Melting Point (°C)
GaAs	5.653	1.428	Direct	1238
GaP	5.451	2.268	Indirect	1467
InP	5.868	1.34	Direct	1062
Si	5.431	1.11	Indirect	1415
Ge	5.646	0.664	Indirect	937

The LEC technique for GaAs consists of a crucible containing a molten GaAs solution, into which a single crystal "seed" is dipped. The temperature is carefully controlled so that the molten GaAs slowly freezes on the seed as the seed is rotated and raised out of the molten solution. By properly controlling the temperature, rotation rate, seed lift rate, etc., the seed can be grown into a single crystal weighing several kilograms and having a diameter of typically 2 to 4 in for GaAs and for 2 to 2.5 in for GaP. At the GaAs and GaP melting points As and P would rapidly evaporate from the growth crucible if they were not contained with a molten boric oxide layer covering the growth solution. This layer is the reason for the name "liquid encapsulated." The seed is dipped through the boric oxide to grow the crystal. The growth chamber must be pressurized to keep the phosphorus and arsenic from bubbling through the boric oxide. The growth pressure for GaP is 80 atm, and for GaAs is 20 atm or less, depending upon the approach for synthesis and growth. The LEC technique, used for GaAs, GaP, and InP, is similar to the Czochralski technique used for silicon, but the silicon process is much simpler since encapsulation is not required and the growth can be done at atmospheric pressure.

The Bridgeman and the gradient-freeze technique, which is a variation of the Bridgeman technique, can also be used to grow compound semiconductors. In this technique the growth solution and seed are contained in a sealed chamber so liquid encapsulation is not required. Growth is accomplished by having a temperature gradient in the solution, with the lowest temperature at the melting point in the vicinity of the seed. Growth can be accomplished by lowering the temperature of the entire chamber (gradient freeze), or by physically moving the growth chamber relative to the furnace (Bridgeman technique) to sweep the temperature gradient through the molten solution. The growing crystal can be in either a vertical or horizontal position.

GaAs for LEDs is commonly grown using either LEC or horizontal gradient freeze, also called "boat grown," but sometimes a vertical Bridgeman approach is used. GaP and InP are almost always grown using LEC but sometimes a vertical Bridgeman approach has also been used.

17.8 EPITAXIAL TECHNOLOGY

Growth Techniques Available

Epitaxial layers are grown using one of several techniques, depending on the material system. The most common techniques are liquid phase epitaxy (LPE), which is primary used to grow GaAs, GaP, and AlGaAs and vapor phase epitaxy (VPE), which is used to grow GaAsP. Metalorganic vapor phase epitaxy (MOVPE) is also used to grow AlGaAs, GaInAsP, and AlInGaP. Molecular beam epitaxy (MBE) is used for lasers and high-speed devices but is not used for high-volume commercial LEDs at this time. It has been used to grow blue ZnSe-based lasers and LEDs and could be important in the future. All of these epitaxial techniques have been discussed extensively elsewhere and will be only briefly described here.

LPE

LPE growth consists of a liquid growth solution, generally gallium, which is saturated with the compound to be grown.[26] The saturated solution is placed in contact with the substrate at the desired growth temperature, and cooled. As the solution cools, an epitaxial film is grown on the substrate. The technique has the advantage that it is relatively easy to grow high-quality epitaxial layers, and materials containing aluminum (such as AlGaAs) can be readily grown. The disadvantages are that composition control can be difficult. Also, the growth of epitaxial structures involving more than two or three layers, particularly thin layers, can be mechanically complicated since each layer requires a separate growth solution that must be carefully saturated and sequentially brought into contact with the substrate.

One important use of the LPE technique has been for the growth of GaP:ZnO and GaP:N for red and green LEDs, respectively. These devices each consist of two relatively thick layers: an *n*-type layer,

followed by the growth of a *p*-type layer. While other growth techniques can be used to grow GaP LEDs, the best results have been obtained using LPE. As a result of a high-volume, low-cost production technology has evolved, which produces more visible LED chips than any other technique. Another major use of LPE is for the growth of GaAs: Si for infrared emitters. LPE is the only technique with which it has been possible to produce the recombination center that gives rise to the 940-nm emission characteristic of this material. The GaAs: Si structures are generally grown from a single growth solution. At high temperatures the silicon is incorporated on Ga sites and the layers are *n* type. As the solution cools the silicon becomes preferentially incorporated on the As sites and the layer becomes *p* type.

AlGaAs devices for both visible (red) and IR devices are also generally grown by LPE. AlGaAs devices can also be grown by MOCVD, but LPE has the advantage that thick layers can be more easily grown. This is important for high extraction efficiency (see under "Device Structures" and Fig. 12). In the case of visible devices at 650 nm, the internal quantum efficiency is also higher using LPE than MOCVD. This is not understood, but the result is that virtually all of the visible AlGaAs LEDs are produced using LPE.

VPE

VPE is the other major commercial epitaxial technology for LEDs.[9,27] VPE consists of a quartz chamber containing the substrate wafers at the appropriate growth temperature. The reactants are transported to the substrates in gaseous form. The technique is mainly used for the growth of GaAsP which, along with GaP, dominates the high-volume visible LED market. In this case HC1 is passed over Ga metal to form gallium chlorides, and AsH_3 and PH_3 are used to provide the As and P compounds. Appropriate dopant gases are added to achieve the *n*- and *p*-type doping. NH_3 is used to achieve nitrogen doping for the growth of GaAsP:N. The VPE technique has the advantages that it is relatively easy to scale up the growth chamber size so large quantities of material can be grown and layer composition and thickness can be easily controlled by adjusting the flow conditions. A limitation of VPE is that it has not been possible to grow high-quality compounds containing aluminum because the aluminum-bearing reactants attack the quartz chamber resulting in contaminated films. Thus, AlGaAs and AlInGaP, the emerging high-brightness technologies, cannot be grown using this technique.

MOCVD

MOCVD growth, like conventional VPE, uses gases to transpose the reactants to the substrates in a growth chamber.[28] However, in this case metallorganic compounds such as trimethylgallium (TMG) are used for one or more of the reactants. A major difference between VPE and MOCVD is that in the case of MOCVD the decomposition of the source gas (e.g., TMG) occurs as a reaction at or near the substrate surface, and the substrate is in the hottest area of the reactor such that the decomposition occurs on the substrate instead of the walls of the growth chamber. The walls of the growth chamber remain relatively cool. This is the key factor that makes MOCVD suitable for the growth of aluminum-bearing compounds which, unlike the VPE situation, do not react significantly with the cooler reactor walls. Thus AlGaAs and AlInGaP can be readily grown with MOCVD, and this technology is widely used for infrared AlGaAs LEDs and lasers, and for the emerging visible AlInGaP laser and LED technology.

MOCVD is also used for the growth of GaN and AlGaN that are candidates for blue emission, and for the growth of II–VI compounds, such as ZnSe, that is also a potential blue emitter. However, at this time the key limitation in obtaining blue ZnSe emitters is the growth of low-resistivity *p*-type ZnSe. For reasons that are not yet understood, low-resistivity *p*-type ZnSe has been grown using MBE only.

MBE

MBE is a high vacuum growth technique in which the reactants are essentially evaporated onto the substrates under very controlled conditions.[29] MBE, like MOCVD, can be used to deposit compounds

containing aluminum. The growth rates using MBE are generally slower than the other epitaxial techniques, so MBE is most suitable for structures requiring thin layers and precise control of layer thickness. MBE equipment is somewhat more expensive than the equipment used for the other types of epitaxial growth, so it has not been suitable for the high-volume, low-cost production that is required for most types of LEDs. MBE has generally been utilized for lasers and high-speed devices where control of complicated epitaxial structures is critical and where relatively low volumes of devices are required. One advantage that MBE has over the other growth technologies is that the reactants utilized are generally less hazardous. Consequently, MBE equipment is often cheaper and easier to install since there are less safety issues and safety-code restrictions to deal with.

17.9 WAFER PROCESSING

Wafer Processing Overview

Wafer processing of compound semiconductors for LED applications has many of the same general steps used to process silicon integrated-circuit wafers, namely passivation, diffusion, metallization, testing, and die fabrication. The LED device structures are much simpler, so fewer steps are required; but, due to the materials involved, the individual steps are generally different and sometimes more complicated.

Compound semiconductor processing has been described in detail elsewhere, so only a brief summary is discussed here.[30] Some types of LED structures require all of the processing steps listed here, but in many cases fewer process steps are required. An example is a GaP or AlGaAs device with a grown *p-n* junction. For these devices no passivation or diffusion is required.

Passivation

Some types of LED structures, particularly multijunction structures, require a passivation layer prior to diffusion, as shown in Fig. 7. This layer must be deposited relatively free of pinholes, be patternable with standard photolithographic techniques, and must block the diffusing element, generally zinc. In the case of silicon, a native oxide is grown which is suitable for most diffusions. Unfortunately, the compound semiconductors do not form a coherent native oxide as readily as silicon. Silicon nitride (Si_3N_4) is the most widely used passivation layer for LEDs. Si_3N_4 is grown by reacting silane (SiH_4) and ammonia at high temperature in a furnace. S_3N_4 blocks zinc very effectively, and is easily grown, patterned, and removed. Sometimes an SiO_2 layer is used in conjunction with Si_3N_4 for applications such as protecting the surface of the compound semiconductor during high-temperature processing. Silicon oxynitride can also be used instead of or in addition to pure Si_3N_4. Silicon oxynitride is somewhat more complicated to deposit and control, but can have superior properties, such as a better match of coefficient of expansion, resulting in lower stress at the interface.

Diffusion

Generally, only *p*-type impurities, usually Zn, are diffused in compound semiconductors. *N*-type impurities have prohibitively small diffusion coefficients for most applications. Zn is commonly used because it diffuses rapidly in most materials and because it is nontoxic in contrast to Be, which also diffuses rapidly. Mg is another reasonable *p*-type dopant, but it diffuses more slowly than zinc. Diffusions are generally done in evacuated and sealed ampoules using metallic zinc as source material. A column V element such as As is also generally added to the ampoule to provide an overpressure that helps to prevent decomposition of the semiconductor surface during diffusion. Diffusion conditions typically range from 600 to 900°C for times ranging from minutes to days, depending upon the material and device involved. Junction depths can range from a fraction of a μm to a more than 10 μm.

Open-tube diffusions have also been employed but have generally been harder to control than the sealed ampoule approach, often because of surface decomposition problems. Open-tube diffusions have the advantage that one does not have to deal with the expense and hazard of sealing, breaking, and replacing quartz ampoules.

A third type of diffusion that has been used is a "semisealed" ampoule approach in which the ampoule can be opened and reused. The diffusion is carried out at atmospheric pressure and the pressure is controlled by having a one-way pressure relief valve on the ampoule.

Contacting

The contacts must make good ohmic contact to both the *p*- and *n*-type semiconductor, and the top surface of the top contact must be well suited for high-speed wire bonding. Generally, multilayer contacts are required to meet these conditions. Evaporation, sputtering, and *e*-beam deposition are all employed in LED fabrication. The *p*-type contact generally uses an alloy of either Zn or Be to make the ohmic contact. An Au-Zn alloy is the most common due to the toxicity of Be. The Au-Zn can be covered with a layer of Al or Au to enable high-yield wire bonding. A refractory metal barrier layer may be included between the Au-Zn and top Al or Au layer to prevent intermixing of the two layers and the out-diffusion of Ga, both of which can have a deleterious effect on the bondability of the Al or Au top layer. The *n*-type contact can be similar to the *p*-type contact except that an element which acts as an *n*-type dopant, commonly Ge, is used instead of Zn. An Au-Ge alloy is probably most frequently used to form the *n*-type ohmic contact since it has a suitably low melting point. If the *n*-type contact is the top, or bonded, contact it will be covered by one or more metallic layers to enhance bondability.

Testing

The key parameters that need to be tested are light output, optical rise and fall times, emission wavelength, forward voltage, and leakage current. The equipment used is similar to that used to test other semiconductor devices except that a detector must be added to measure light output. Rise and fall times and wavelength are generally measured on only a sample basis and not for each device on a wafer. In order to test the individual LEDs, the devices must be isolated on the wafer. This occurs automatically for LEDs that are masked and diffused, but if the LEDs are sheet diffused or have a grown junction, the top layer must be processed to isolate individual junctions. This can be accomplished by etching or sawing with a dicing saw. Generally, sawing is used, followed by an etch to remove saw damage, because the layers are so thick that etching deep (>10 μm) grooves is required. It is advisable to avoid deep groove etching because undercutting and lateral etching often occur and the process becomes hard to control. In many cases LED junctions are not 100 percent tested. This is particularly true of GaP and AlGaAs red-emitting devices in which the top layer may be 30 μm thick. Wafers of this type can be sampled by "coring" through the top layer of the wafer in one or more places with an ultrasonic tool in order to verify that the wafer is generally satisfactory. Later, when chips are fully processed, chips can be selected from several regions of the wafer and fully tested to determine if the wafer should be used or rejected.

Die Fab

Die fab is the process of separating the wafer into individual dice so they are ready for assembly. Generally, the wafer is first mounted on a piece of expandable tape. Next the wafer is either scribed or sawed to form individual dice. Mechanical diamond scribing or laser scribing were the preferred technologies in the past. Mechanical scribing has zero kerf loss, but the chips tend to have jagged edges and visual inspection is required. Laser scribing provides uniform chips but the molten waste material from between the chips damages neighboring chips, and in the case of full function chips

the edges of the junction can be damaged by the laser. As a result of the limitations of scribing, sawing (using a dicing saw with a thin diamond impregnated blade) has become the technology of choice for most LEDs.

The kerf loss for sawing has been reduced to about 40 μm and the chip uniformity is excellent such that a minimum of inspection and testing is required. For most materials a "cleanup" etch is required after sawing to remove work damage at the edges of the chips, which can both affect the electrical performance and absorb light. The wafer remains on the expandable tape during the sawing process. After sawing, the tape is expanded so that the chips are separated. The tape is clamped in a ring that keeps it expanded and the chips aligned. In this form the chips are easily individually picked off the tape by the die-attach machine that places the chips in the LED package.

17.10 LED QUALITY AND RELIABILITY

LEDs offer many advantages over other types of light sources. They have long operating life, they operate over a wide temperature range, and they are unaffected by many adverse environmental conditions. LED devices also are mechanically robust, making them suitable for applications where there is high vibration, shock, or acceleration. Excellent quality and reliability are obtainable when an LED product is properly designed, fabricated, packaged, tested, and operated.

Product quality is defined as "fitness for use" in a customer's application. Quality is measured in units of the average number of defective parts per million shipped (i.e., ppm), and is inferred from product sampling and testing. LED product quality is assured by (1) robust chip and product design, (2) high-quality piece parts, (3) well-controlled fabrication processes, (4) use of statistical process control during manufacturing, (5) careful product testing, and (6) proper handling and storage. Most III–V LEDS are comparable in quality to the best silicon devices manufactured today. Well-designed LED products have total defect levels well below 100 ppm.

Reliability measures the probability that a product will perform its intended function under defined use conditions over the useful life of the product. Probability of survival is characterized by a failure rate, which is calculated by dividing the number of failures by the total number of operating hours (number of products tested per x hours operated). Common measures for reliability are percent failures per 1000 hours (percent/khr) and number failures per 10^9 hours (FITS). LED failure rates typically are better than 0.01 percent per khr at 50°C.

The reliability of an LED product is dependent on the reliability of the LED semiconductor chip and on the robustness of the package into which the chip is placed. Interactions between the chip and package can affect product reliability as well. Aspects of LED packaging and LED chip reliability are discussed in the following paragraphs.

LED Package Reliability

The package into which the LED chip is assembled should provide mechanical stability, electrical connection, and environmental protection. To evaluate package integrity, stress tests such as temperature cycling, thermal and mechanical shock, moisture resistance, and vibration are used to establish the worst-case conditions under which a product can survive. Generally, product data sheets contain relevant information about safe conditions for product application and operation.

Plastic materials are commonly used to package LEDs (see under "LED-Based Products"). Thermal fatigue is a limiting factor in plastic-packaged LEDs. Take the case of the plastic LED lamp shown later in Fig. 21. Because of the different materials used (epoxy plastic, copper lead frame, gold wire, III–V LED, etc.) and the different coefficients of expansion of these materials, temperature changes cause internal stresses. If the package is not well designed and properly assembled, thermal changes can cause cracking, chip-attach failure, or failure of the wire bond (open circuits). Careful design can reduce these problems to negligible levels over wide temperature ranges. Today's high-quality plastic lamps are capable of being cycled from −55 to +100°C for 100 cycles without failure.

Long-term exposure to water vapor can lead to moisture penetration through the plastic, subjecting the chips to humidity. High humidity can cause chip corrosion, plastic delamination, or surface leakage problems. Plastic-packaged LEDs are typically not harmed when used under normal use conditions. Accelerated moisture resistance testing can be used to test the limits of LED packages. Plastic materials have been improved to the point that LED products can withstand 1000 hours of environmental testing at elevated temperatures and high humidity (i.e., 85°C and 85 percent RH).

The thermal stability of plastic packaging materials is another important parameter. Over normal service conditions, the expansion coefficient of plastic is relatively constant. Above the so-called glass transition temperature T_g the coefficient increases rapidly. Reliable operation of plastic-packaged LEDs generally requires operation at ambient temperatures below T_g. Failures associated with improper soldering operations, such as too high a soldering temperature or for too long a time can cause the package to fail. Excessive storage temperatures also should be avoided. When an LED product is operated, internal ohmic heating occurs; hence, the safe operating maximum temperature is generally somewhat lower than the safe storage temperature.

LED Chip Reliability

The reliability characteristics of the LED chip determine the safe limits of operation of the product. When operated at a given temperature and drive current there is some probability that the LED will fail. In general, LED failure rates can be separated into three time periods: (1) infantile failure, (2) useful life, and (3) the wearout period (see Fig. 18). During the infant mortality period, failures occur due to weak or substandard units. Typically, the failure rate decreases during the infantile period until no weak units remain. During the "useful life" period, the failure rate is relatively low and constant. The number of failures that do occur are random in nature and cannot be eliminated by more testing. The useful life of an LED is a function of the operating temperature and drive conditions. Under normal use conditions, LEDs have useful lives exceeding 100,000 hours. The wearout period is characterized by a rapidly rising failure rate. Generally, wearout for LEDs is not a concern, as the useful life far exceeds the useful life of the product that the LEDs are designed into.

The principle failure mode for LED chips is light-output degradation. In the case of a visible lamp or display, failure is typically defined as a 50 percent decrease in light output from its initial

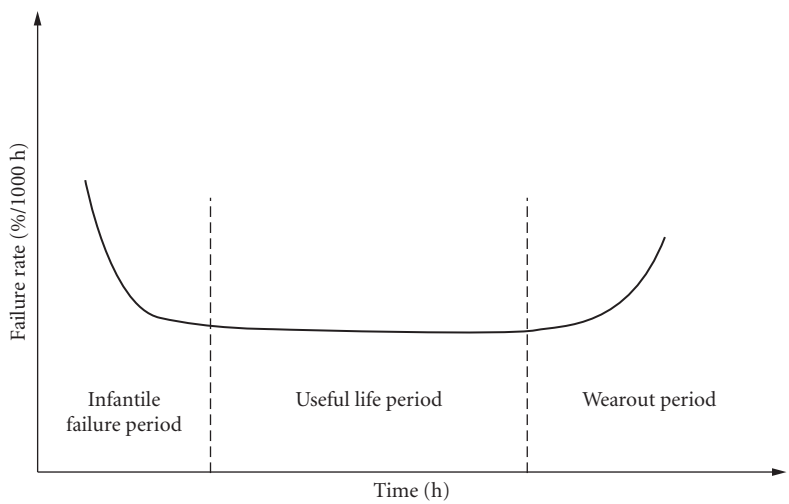

FIGURE 18 Plot of LED failure rate versus time, showing the infantile failure period (decreasing rate), the useful life period (constant, low rate), and the wear-out period (rapidly rising rate).

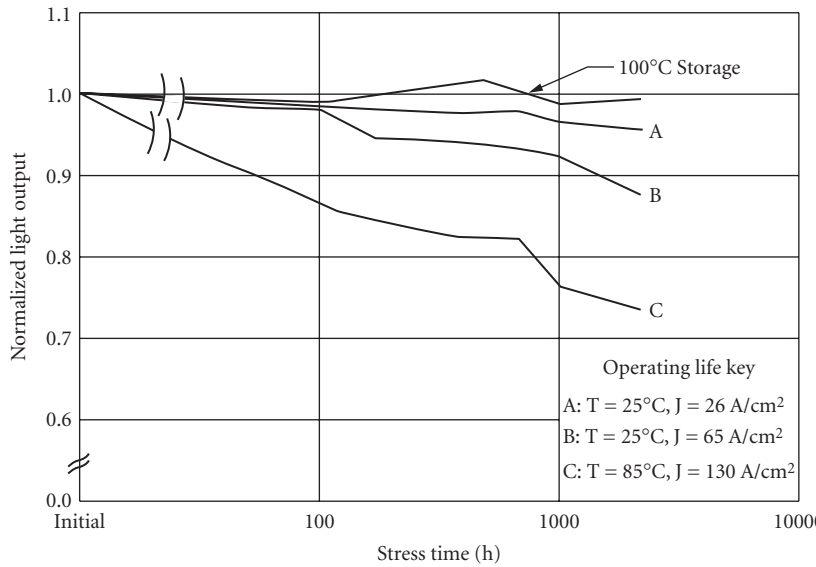

FIGURE 19 Curves of light output versus time for GaAsP indicator lamps stressed under various conditions. Light output is normalized to the initial value. Each curve shows the average degradation of 20 lamps

value, since that is the level where the human eye begins to observe a noticeable change. For infrared emitters or visible LEDs where flux is sensed by a semiconductor detector, failure is commonly defined as a 20 to 30 percent decrease in flux output.

Figure 19 shows degradation curves for a direct bandgap GaAsP LED packaged in a 5-mm plastic lamp.[31] Current must flow for degradation to occur, as negligible change is observed after 1 khr of 100°C storage. Degradation is a function of the temperature at the *p-n* junction and the junction current density. As shown in Fig. 19, a larger decline in light output is observed as junction current density and/or temperature at the junction increases. The dependence of degradation on current density J is superlinear, varying as J^x with $1.5 < x < 2.5$. Hence, accelerated-aging tests typically use high currents and temperatures to shorten the time needed to observe LED degradation. The maximum stress level shown in Fig. 19 is 200 percent of the maximum allowable drive current specified in the data sheet.

Light-output degradation in GaAsP LEDs is due to an increase in the nonradiative space-charge recombination current. Total current flowing through the LED is made up of the sum of diffusion current and space-charge recombination current, as shown in the following equations:

$$I_T(V,t) = A(t)e^{qV/kT} + B(t)e^{qV/2kT} \tag{5}$$

where q is electron charge, k is Boltzmann's constant, and T is temperature.[32] The first term is diffusion current that produces light output, while the second term is space-charge recombination that is nonradiative. At fixed I_T, if $B(t)$ increases, then the diffusion term must decrease and, hence, the light output decreases. The reason for the increase in space-charge recombination in GaAsP LEDs is not fully understood.

The degradation characteristics of GaAlAs LEDs differ from those of GaAsP LEDs. Typical curves of normalized light output versus time for GaAlAs LEDs are shown in Fig. 20. "Good" units show negligible decrease in light output when operated under normal service conditions. Gradual degradation may occur, but it is relatively uncommon. The predominate failure mode in GaAlAs LEDs is catastrophic degradation. The light emission decreases very rapidly over a period of less than 100 hours

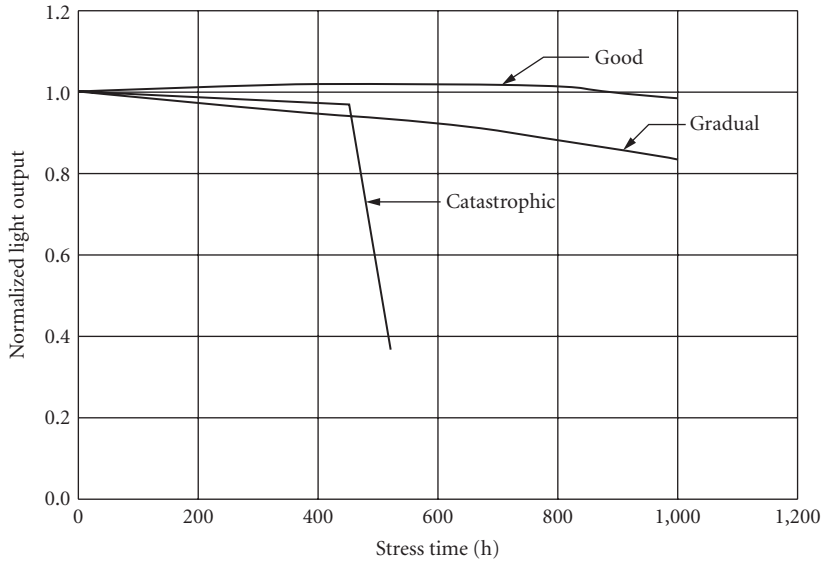

FIGURE 20 Light output degradation of AlGaAs LEDs. Three modes are shown: "good" devices with negligible light-output decrease over time, devices which degrade gradually over time, and "catastrophic" degradation devices where the flux rapidly decreases over a short time period

and simultaneously nonradiative regions ("dark-spot" or "dark-line defects") are observed to form. The catastrophic degradation mechanism is described in detail in Refs. 33 and 34. In brief, the dark regions are caused by nonradiative recombination at dislocation networks that grow rapidly from a crystal dislocation located in the light-emitting region of the LED. Network formation depends on carrier recombination, both nonradiative, which creates mobile point defects, and radiative recombination, which enhances the movement of the point defects to the growing network.

Formation of dark-line defects is enhanced by mechanical stress either present in the LED chip or occurring during assembly. Properly designed products reduce such stress by minimizing bending caused by the different coefficients of expansion in the LED, and by stress-free die attach, wire bond, and encapsulation of the LED during assembly.

Failures due to dark-spot or dark-line defects can be effectively screened out by operating the LED at high current and temperature. Units with defects typically fail within the first few hundred hours. GaAlAs LEDs with dark-spot or dark-line defects are screened out by means of visual inspection and/or by eliminating units with large decreases in light output. GaAlAs LEDs used for fiber-optic applications have small emitting areas (see under "Fiber Optics" discussion and Fig. 14). Due to the high current densities present in such devices, high temperature and current burn-in is used extensively for these types of LEDs.

Another degradation mode in LEDs is the change in the reverse breakdown characteristics over time. The reverse characteristics become soft and the breakdown voltage may decrease to a very low value. Several mechanisms have been observed in LEDs. One cause is localized avalanche breakdown due to microplasma formation at points where electric fields are high. Microplasmas have been observed in GaAs and GaAsP LEDs.

Damage or contamination of the edges of an LED chip can cause increased surface leakage and reduced reverse breakdown. Incomplete removal of damage during die separation operations and damage induced during handling and assembly are known to cause reverse breakdown changes. Die-attach materials also can unintentionally contaminate the edges of LEDs. Copper, frequently found in LED packaging materials, can diffuse into the exposed surfaces of the LED, causing excess leakage and, in some cases, light-output degradation.[35] Chips whose *p-n* junction extends to the edges (i.e., Fig. 6) are very susceptible to damage and/or contamination.

17.11 LED-BASED PRODUCTS

Indicator Lamps

The simplest LED product is an indicator lamp or its infrared equivalent. The most frequently used lamp is shown in Fig. 21. A LED chip with a typical dimension of 250 × 250 μm is attached with conductive silver-loaded epoxy into a reflective cavity coined into the end of a silver-plated copper or steel lead frame. The top of the LED chip is connected with a thin 25-μm gold wire to the second terminal of the lead frame. The lead frame subassembly is then embedded in epoxy. The epoxy serves several functions: (1) it holds the assembly together and protects the delicate chip and bond wire; (2) it increases the light extraction from the chip (see under "Light Extraction," discussed earlier); and (3) it determines the spatial light distribution.

There are a large number of variations of the lamp shown in Fig. 21. Besides the obvious variation of source wavelength, there are variations of size, shape, radiation pattern, etc. The cross section of the plastic body ranges from 2 to 10 mm. The radiation pattern is affected by three factors: the shape of the dome, the relative position of the chip/reflector combination, and by the presence of a diffusant in the epoxy. Figure 22*a* shows the radiation pattern of a lamp using clear plastic as an encapsulant. The rays emanating from chip and reflector are collimated into a narrow beam. For many indicator lamps a broader viewing angle is desired such as that shown in the radiation pattern of Fig. 22*b*. This effect is achieved by adding a diffusant, such as glass powder, to the clear plastic. Another variation is shape. Common shapes are round, square, rectangular, or triangular.

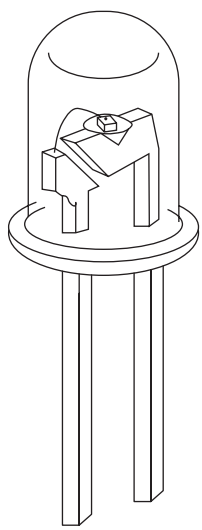

FIGURE 21 Plastic indicator lamp. The LED chip is placed in a reflector coined into the end of one electrode lead. The top of the chip is connected with a gold wire to the second electrode. The electrodes are encapsulated in plastic to form a mechanically robust package.

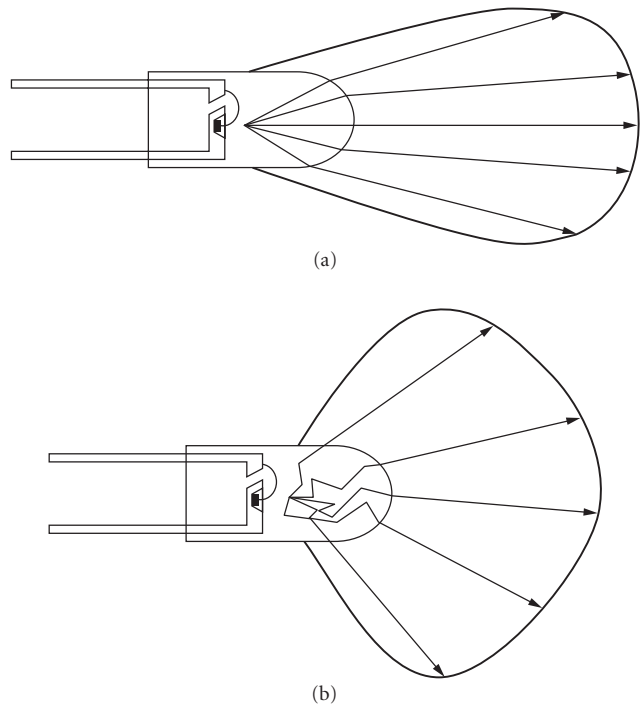

FIGURE 22 Radiation pattern of two types of LED indicator lamps: *(a)* lamp with clear plastic package with a narrow beam and *(b)* lamp with a diffusing plastic package (glass powder added) with a broader radiation pattern.

Another variation is achieved by placing two different chips into the reflector cup. For instance, a lamp with green and red chips connected to the second post in an antiparallel fashion can operate as a red indicator if the reflector post is biased positive, and as a green indicator if it is biased negative. Rapidly switching between the two polarities one can achieve any color between the two basic colors, i.e., yellow or orange, depending on current and duty cycle.

A number of chips can be combined in a single package to illuminate a rectangular area. These so-called annunciator assemblies range in size from 1 to several cm. They typically use 4 chips per cm^2. By placing an aperture-limiting symbol or telltale in front of the lit area, these structures are cost-effective means to display a fixed message, such as warning lights in an automotive dashboard.

Numeric Displays

Numeric displays are usually made up of a nearly rectangular arrangement of seven elongated segments in a figure-eight pattern. Selectively switching these segments generates all ten digits from 0 to 9. Often decimal point, colon, comma, and other symbols are added.

There are two main types of LED numeric displays: (1) monolithic displays and (2) stretched segment displays. All monolithic displays are based on GaAs-GaAsP technology. Seven elongated *p*-doped regions and a decimal point are diffused into an *n*-type epitaxial layer of a single or monolithic chip (see Fig. 8). Electrically, this is a structure with eight anodes and one common cathode. This monolithic approach is relatively expensive. For arms-length viewing, a character height of 3 to 5 mm is required. Adding space for bonding pads, decimal point, and edge separation, such a display consumes around 10 mm^2 of expensive semiconductor material per digit. One way to reduce material and power consumption is optical magnification. Viewing-angle limitation and distortion limit the magnification M to $M \leq 2.0$. Power consumption is reduced by M^2—an important feature for battery-powered applications.

For digits >5 mm, a stretched segment display is most cost effective. The design of Fig. 23 utilizes a 250 × 250 μm chip to generate a segment with dimensions of up to 8 × 2 mm for a 20-mm digit height. This corresponds to a real magnification of $M^2 = 256$, or an equivalent linear magnification of $M = 16$. This magnification is achieved without a reduction in viewing angle by using scattering optics. An LED chip is placed at the bottom of a cavity having the desired rectangular exit shape and

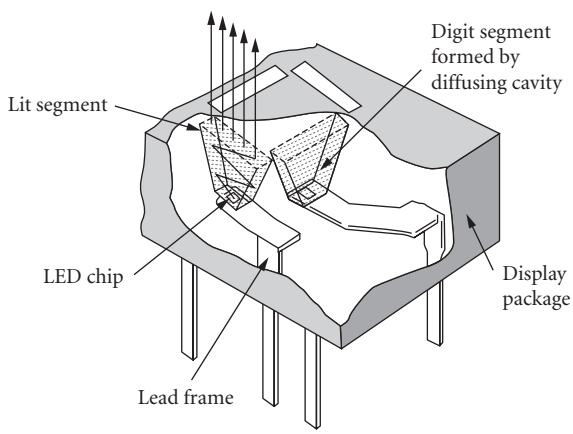

FIGURE 23 Cutaway of a seven-segment numeric LED display, showing how light from a small LED chip is stretched to a large character segment using a diffusing cavity. Characters 0 to 9 are created by turning on appropriate combinations of segments.

LIGHT-EMITTING DIODES

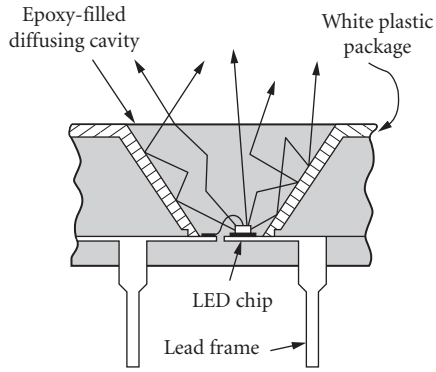

FIGURE 24 Cross section through one segment of the seven-segment numeric display shown in Fig. 23. A LED chip is placed at the bottom of a highly reflective, white plastic cavity which is filled with clear plastic containing a diffusant. Light is scattered within the cavity to produce uniform emission at the segment surface.

the cavity is filled with a diffusing plastic material (see Fig. 24). The side and bottom surfaces of the cavity are made as reflective as possible. Highly reflective white surfaces are typically used. A good white plastic surface measured in air may have a reflectivity of 94 percent compared with 98 percent for Ag and 91 percent for Al. Ag and Al achieve this reflectivity only if evaporated on a specularly smooth surface. Measured in plastic, the reflectivity of the white surface increases from 94 to 98 percent, the Ag surface remains at 98 percent, while the Al surface decreases to 86 percent. Both metallic surfaces have substantially lower reflectivities if they are evaporated onto a nonspecular surface, or if they are deposited by plating. Practically all numeric LED displays above 5-mm character heights are made using white cavity walls and diffusing epoxy within the cavity.

This case of magification by scattering does not result in a power saving as in the case of magnification of monolithic displays. Since there is practically no reduction in emission angle, the law of energy conservation requires an increased light flux from the chip that equals the area magnification plus reflection losses in the cavity.

Alphanumeric Displays

There are two ways LEDs are used to display alphanumeric information: either by using more than seven elongated segments, i.e., 14, 16, or 24; or by using an array of LED chips in a 5×7 dot matrix format. The multiple segment products are similar in design to the monolithic or stretched segment numeric displays described above.

In the case of small monolithic characters, the number of input terminals quickly exceeds conventional pin spacing. These products are usually clusters of 4 to 16 characters combined with a decoder/driver integrated circuit within the same package. To reduce cost and power, some modest optical magnification is usually used. The segmented displays are usually larger, i.e., 12 to 25 mm and limited to 14 segments per character. At this size, there is no pin density constraint and the decoder is usually placed outside the package.

The most frequently used alphanumeric LED display is based on a 5×7 matrix per character. For small characters in the range of 5 to 8 mm, the LED chips are directly viewed and pin density limitations require an on-board decoder/driver IC. Products are offered as end-stackable clusters of 4, 8, and 16 characters.

For larger displays, the LED chip is magnified by the same optical scattering technique described earlier for numerics. Exit apertures per pixel have a diameter of 2 to 5 mm. Products are offered as 5×7 single characters or end-stackable 20×20 tiles for large message- or graphics-display panels. At this size, pin density is not a limitation.

Optocouplers

An optocoupler is a device where signal input and signal output have no galvanic connection. It is mainly used in applications as the interface between the line voltage side of a system and the low-voltage circuit functions, or in systems where the separate ground connection of interconnected subsystems causes magnetic coupling in the galvanic loop between signal and ground connections. By interrupting the galvanic loop with an optical signal path, many sources of signal interference are eliminated.

The oldest optocouplers consist of an IR LED and a photodetector facing each other in an insulating tube. The second generation utilized the so-called dual-in-line package widely used by logic ICs. In this package an IR emitter and a phototransistor are mounted face to face on two separate lead frames. The center of the package between emitter and detector is filled with a clear insulating material. The subassembly is then molded in opaque plastic to shield external light and to mechanically stabilize the assembly (Fig. 25). The second generation optocouplers have limited speed performance for two reasons: (1) the slow response time of the GaAs:Si LED and (2) the slow response of the photo-transistor detector because of the high collector-base capacitance.

The third generation of optocouplers overcomes the speed limitation. It uses an integrated photodetector and a decoupled gain element. Integration limits the thickness of the effective detection region in silicon to 5 to 7 μm. This thickness range forces a shift of the source to wavelengths shorter than the 940-nm sources used in the second-generation couplers. Third-generation couplers use GaAsP (700 nm) or AlGaAs emitters (880 nm).

Within the last decade, the optocoupler product family has seen further proliferation by adding features on the input or output side of the coupler. One proliferation resulted in couplers behaving

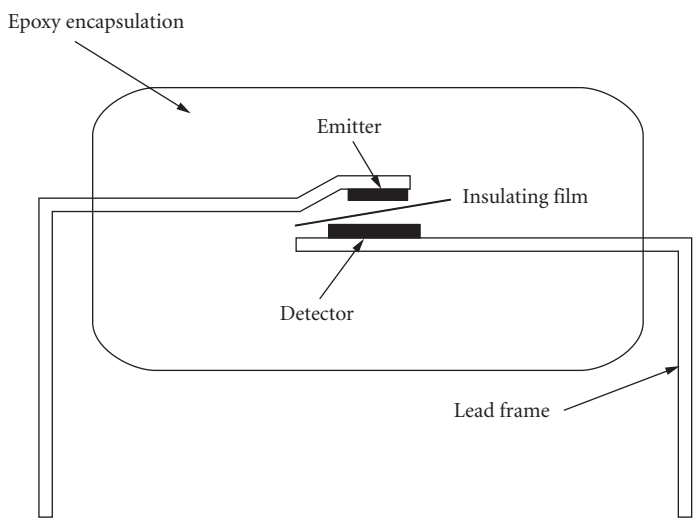

FIGURE 25 Optocoupler consisting of face-to-face emitter and detector chips. An insulating film is placed between the chips to increase the ability of the optocoupler to withstand high voltages between input and output electrodes

like logic gates. Another variation used MOS FET devices on the output side, eliminating the offset voltages of bipolar devices. These couplers are comparable to the performance of conventional relays and are classified as solid-state relays. Other types use a CMOS input driver and CMOS output circuitry to achieve data transfer rates of 50 Mb/s and CMOS interface compatibility.

Fiber Optics

LEDs are the primary light source used in fiber-optic links for speeds up to 200 Mb/s and distances up to 2 km. For higher speed and longer distances, diode lasers are the preferred source.

For fiber-optic applications, LEDs have to meet a number of requirements that go well beyond the requirements for lamps and displays. The major issues are minimum and maximum flux coupled into the fiber, optical rise and fall times, source diameter, and wavelength. Analysis of flux budget, speed, fiber dispersion, wavelength, and maximum distance is quite complex and goes far beyond the scope of this work. A simplified discussion for the popular standard, Fiber Distributed Data Interface (FDDI) will highlight the issues. For a detailed discussion, the reader is referred to Ref. 36.

Flux Budget The minimum flux that has to be coupled into the fiber is determined by receiver sensitivity (−31 dBm), fiber attenuation over the 2-km maximum distance (3 dB), connector and coupler losses (5 dB), and miscellaneous penalties for detector response variations, bandwidth limitations, jitter, etc. (3 dB). With this flux budget of 11 dB, the minimum coupled power has to be −20 dBm. Another flux constraint arises from the fact that the receiver can only handle a maximum level of power before saturation (−14 dBm). These two specifications bracket the power level coupled into the fiber at a minimum of −20 dBm (maximum fiber and connector losses) and at a maximum of −14 dBm (no fiber or connector losses for the case of very short fiber).

Speed The transmitter speed or baud rate directly translates into a maximum rise and fall time of the LED. The 125 Mdb FDDI specifications call for a maximum rise and fall time of 3.5 ns. As a rule of thumb, the sum of rise and fall time should be a little shorter than the inverse baud period (8 ns for 125 Mbd).

Source Diameter and Fiber Alignment Efficient coupling of the LED to the fiber requires a source diameter that is equal to or preferably smaller than the diameter of the fiber core. For sources smaller than the core diameter, a lens between source and fiber can magnify the source to a diameter equal to or larger than the core diameter. The magnification has two benefits: (1) It increases the coupling efficiency between source and fiber. The improvement is limited to the ratio of source area to core cross-sectional area. (2) It increases the apparent spot size to a diameter larger than the fiber core. This effect relaxes the alignment tolerance between source and core and results in substantially reduced assembly and connector costs.

Wavelength The LEDs used in fiber-optic applications operate at three narrowly defined wavelength bands 650, 820 to 870, and 1300 nm, as determined by optical fiber transmission characteristics.

650 nm This band is defined by an absorption window in acrylic plastic fiber. It is a very narrow window between two C-H resonances of the polymer material. The bottom of the window has an absorption of approximately 0.17 dB/m. However, the effective absorption is in the 0.3 to 0.4 dB/m range because the LED linewidth is comparable to the width of the absorption window and the LED wavelength changes with temperature. The 650-nm LEDs use either $GaAs_{1-x}P_x$ with $x = 0.4$ or $GaAl_xAs_{1-x}$ with $x = 0.38$. Quantum efficiencies are at 0.2 and 1.5 percent, respectively. Maximum link length is in the range of 20 to 100 m, depending on source efficiency, detector sensitivity, speed, and temperature range.

820 to 870 nm This window was chosen for several reasons. GaAlAs emitters (see Fig. 14) and Si detectors are readily available at this wavelength. Early fibers had an absorption peak from water

contamination at approximately 870 nm. As fiber technology improved, the absorption peak was eliminated and the wavelength of choice moved from 820- to the 850 to 870-nm range. Fiber attenuation at 850 nm is typically 3 dB/km. Maximum link length in the 500- to 2000-m range, depending on data rate. In the 850 to 870-nm window the maximum link length is limited by chromatic dispersion. GaAlAs emitters have a half-power linewidth of approximately 35 nm. The velocity of light in the fiber is determined by the index of refraction of the fiber core. The index is wavelength-dependent resulting in dispersion of the light pulse. This dispersion grows with distance. The compounded effect of LED linewidth and fiber dispersion is a constant distance-speed product. For a typical multimode fiber and GaAlAs LED combination, this product is in the range of 100 Mbd-km.[36]

1300 nm At this wavelength, the index of refraction as a function of wavelength reaches a minimum. At this minimum, the velocity of light is practically independent of wavelength, and chromatic dispersion is nearly eliminated. The distance-speed limitation is caused by modal dispersion. Modal dispersion can be envisioned as a different path length for rays of different entrance angles into the fiber. A ray going down the middle of the core will have a shorter path than a ray entering the fiber at the maximum acceptance angle undergoing many bends as it travels down the fiber. The resulting modal dispersion limits multimode fibers to distance bandwidth products of approximately 500 Mbd-km. LED sources used at this wavelength are GaInAsP emitters, as shown in Fig. 15. At this wavelength, fiber attenuation is typically <1.0 dB/km and maximum link length is in the range of 500 to 5000 m, depending on data rate and flux budget.

Sensors

LED/detector combinations are used in a wide range of sensor applications. They can be grouped into three classes: transmissive, reflective, and scattering sensors.

Transmissive Sensors The most widely used transmissive sensor is the slot interrupter. A U-shaped plastic holder aligns an emitter and detector face to face. It is used widely for such applications as sensing the presence or absence of paper in printers, end-of-tape in tape-recorders, erase/overwrite protection on floppy disks, and many other applications where the presence or absence of an opaque obstruction in the light path determines a system response.

A widely used slot interrupter is a two- or three-channel optical encoder. A pattern of opaque and transmissive sections moves in front of a fixed pattern with the same spatial frequency. Two optical channels positioned such that they are 90° out of phase to each other with regard to the pattern allow the measurement of both distance (number of transmissive/opaque sequences) and direction (phase of channel A with regard to channel B). Such encoders are widely used in industrial control applications, paper motion in printers, pen movement in plotters, scales, motor rotation, etc. A third channel is often used to detect an index pulse per revolution to obtain a quasi-absolute reference.

Reflective Sensors In a reflective sensor an LED, detector, and associated optical elements are positioned such that the detector senses a reflection when a reflective surface (specular or diffuse) is positioned within a narrow sensing range. A black surface or nonaligned specular surface or the absence of any reflective surface can be discriminated from a white surface or properly aligned specular surface. Applications include bar-code reading (black or white surface), object-counting on a conveyer belt (presence or no presence of a reflecting surface), and many others. Many transmissive sensor applications can be replaced by using reflective sensors and visa versa. The choice is usually determined by the optical properties of the sensing media or by cost. An emerging application for reflective sensors is blood gas analysis. The concentration of O_2 or CO_2 in blood can be determined by absorption at two different LED wavelengths, i.e., red and infrared.

Scattering Sensors One design of smoke detectors is based on light scattering. The LED light beam and the detector path are crossed. In the absence of smoke, no light from the LED can reach the detector. In the presence of smoke, light is scattered into the detector.

17.12 REFERENCES

1. A. A. Bergh and P. J. Dean, "Light-Emitting Diodes," *Proc. IEEE* vol. 60, 1972, pp. 156–224.
2. K. Gillessen and W. Shairer, *LEDs—An Introduction,* Prentice-Hall, 1987.
3. M. G. Craford, "Properties and Electroluminescence of the GaAsP Ternary System," *Progress in Solid State Chemistry,* vol. 8, 1973, pp. 127–165.
4. A. H. Herzog, W. O. Groves, and M. G. Craford, "Electroluminescence of Diffused $GaAs_{1-x}P_x$ Diodes with Low Donor Concentrations," *J. Appl. Phys.* vol. 40, 1969, pp. 1830–1838.
5. R. A. Faulkner, "Toward a Theory of Isoelectronic Impurities in Semiconductors," *Phys. Rev.* vol. 175, 1968, pp. 991–1009.
6. W. O. Groves, A. J. Herzog, and M. G. Craford, "The Effect of Nitrogen Doping on $GaAs_{1-x}P_x$ Electroluminescent Diodes," *Appl. Phys. Lett.* vol. 19, 1971, pp. 184–186.
7. M. G. Craford, R. W. Shaw, W. O. Groves, and A. H. Herzog, "Radiative Recombination Mechanisms in GaAsP Diodes with and without Nitrogen Doping," *J. Appl. Physics* vol. 43, 1972, pp. 4075–4083.
8. M. G. Craford, D. L. Keune, W. O. Groves, and A. H. Herzog, "The Luminescent Properties of Nitrogen Doped GaAsP Light Emitting Diodes," *J. Electron. Matls.* vol. 2, 1973, pp. 137–158.
9. M. G. Craford and W. O. Groves, "Vapor Phase Epitaxial Materials for LED Applications," *Proc. IEEE* vol. 61, 1973, pp. 862–880.
10. J. C. Campbell, N. Holonyak Jr., M. G. Craford, and D. L. Keune, "Band Structure Enhancement and Optimization of Radiative Recombination in $GaAs_{1-x}P_x$:N (and $In_{1-x}Ga_xP$:N)," *J. Appl. Phys.* vol. 45, 1974, pp. 4543–4553.
11. R. A. Logan, H. G. White, and W. Wiegmann, "Efficient Green Electroluminescence in Nitrogen-Doped GaP *p-n* Junctions," *Appl. Phys. Lett.* vol. 13, 1968, p. 139.
12. A. A. Bergh and J. A. Copeland, "Optical Sources for Fiber Transmission Systems," *Proc. IEEE,* vol. 68, 1980, pp. 1240–1247.
13. M. G. Craford, "Recent Developments in Light-Emitting Diode Technology," *IEEE Trans. Electron Devices* vol. 24, 1977, pp. 935–943.
14. H. Nather, V. Nitsche, and W. Schairer, "High Resolution Printing Capability of LED-Based Print Heads," *Proc. SPIE,* 1988, pp. 396–404.
15. M. G. Craford, "Light-Emitting Diode Displays," in *Flat-Panel Displays and CRTs,* L. E. Tannas Jr. (ed.), Van Nostrand Reinhold, 1985, pp. 289–331.
16. L. W. Cook, M. D. Camras, S. L. Rudaz, and F. M. Steranka, "High Efficiency 650 nm Aluminum Gallium Arsenide Light Emitting Diodes," *Proc. 14th International Symposium on GaAs and Related Compounds,* Institute of Physics, Bristol, 1988, pp. 777–780.
17. J. M. Dallesasse, D. W. Nam, D. G. Deppe, N. Holonyak Jr., R. M. Fletcher, C. P. Kuo, T. D. Osentowski, and M. G. Craford, "Short-Wavelength (<6400 Å) Room Temperature Continuous Operation of *p-n* InAlGaP Quantum Well Lasers," *Appl. Phys. Lett.* vol. 19, 1988, pp. 1826–1828.
18. C. P. Kuo, R. M. Fletcher, T. D. Osentowski, M. C. Lardizabel, and M. G. Craford, "High Performance AlGaInP Visible Light-Emitting Diodes," *Appl. Phys. Lett.* vol. 57, 1990, pp. 2937–2939.
19. H. Sugawara, M. Ishikawa, and G. Hatakoshi, "High-efficiency InGaAlP/GaAs Visible Light-Emitting Diodes," *Appl. Phys. Lett.* vol. 58, 1991, 1010–1012.
20. R. M. Fletcher, C. P. Kuo, T. D. Osentowski, K. H. Huang, and M. G. Craford, "The Growth and Properties of High Performance AlGaInP Emitters Using a Lattice Mismatched GaP Window Layer," *Jour. Elec. Matls.* vol. 20, 1991, pp. 1125–1130.
21. K. H. Huang, J. G. Yu, C. P. Kuo, R. M. Fletcher, T. D. Osentowski, L. J. Stinson, A. S. H. Liao, and M. G. Craford, "Twofold Efficiency Improvement in High Performance AlGaInP Light- Emitting Diodes in the 555–620 nm Spectral Region Using a Thick GaP Window Layer," *Appl. Phys. Lett.* vol. 61, 1992, pp. 1045–1047.
22. M. A. Haase, J. Qiv, J. M. DePoydt, and H. Cheng, "Blue-green Laser Diodes," *Appl. Phys. Lett.* vol. 58, 1991, pp. 1272–1275.
23. J. Jeon, J. Ding, A. V. Normikko, W. Xie, M. Kobayashi, and R. L. Gunshore, "ZnSe Based Multilayer *p/n* Junctions as Efficient Light Emitting Diodes for Display Applications," *Appl. Phys. Lett.* vol. 60, 1992, pp. 892–894.

24. S. Nakamura, M. Senoh, and T. Mukai, "Highly *P*-typed Mg-doped GaN Films Grown with GaN Buffer Layers," *Jpn. Jour. Appl. Phys.* vol. 30, 1991, pp. L1701–L1711.
25. A. G. Fischer, "Methods of Growing Crystals under Pressure," in *Crystal Growth,* B. R. Pamplin (ed.), Pergamon Press, Oxford, 1975, pp. 521–555.
26. R. L. Moon, "Liquid Phase Epitaxy," in *Crystal Growth,* 2d ed., B. R. Pamplin (ed.), Pergamon Press, Oxford, 1980.
27. J. W. Burd, "A Multi-Wafer Growth System for the Epitaxial Deposition of GaAs and $GaAs_{1-x}P_x$," *Trans. Met. Soc. AIME,* 1969, pp. 571–576.
28. G. B. Stringfellow, *Organometallic Vapor Phase Epitaxial Growth of III-V Semiconductor: Theory and Practice,* Academic Press, Oxford, 1989.
29. E. C. H. Parker (ed.), *Technology and Physics of Molecular Beam Epitaxy,* Plenum Press, New York, 1985.
30. S. K. Ghandhi, *VLSI Fabrication Principles,* John Wiley and Sons, New York, 1982.
31. Hewlett-Packard, *Optoelectronics/Fiber-Optics Application Manual,* 2d ed., McGraw-Hill, New York, 1981, p. 82.
32. A. S. Grove, *Physics and Technology of Semiconductor Devices,* sec. 6.6, John Wiley, New York, 1967.
33. O. Veda, *Material Research Society Symposium Proc.* vol. 184, 1991, p. 125.
34. M. Fukuda, *Reliability and Degradation of Semiconductor Lasers and LEDs,* Artech House, 1991.
35. A. A. Bergh, "Bulk Degradation of GaP Red LEDs," *IEEE Trans. Electron Devices* vol. 18, 1971, pp. 166–170.
36. D. C. Hanson, "Progress in Fiber Optic LAN and MAN Standards," *IEEE LCS Magazine* vol. 1, 1990, pp. 17–25.